ISSN 0024-4902, Lithology and Mineral Resources, 2014, Vol. 49, No. 6, pp. 433–460. © Pleiades Publishing, Inc., 2014.
Original Russian Text © A.V. Maslov, V.P. Shevchenko, V.N. Podkovyrov, Yu.L. Ronkin, O.P. Lepikhina, A.N. Novigatsky, A.S. Filippov, N.V. Shevchenko, 2014, published in Litologiya i Poleznye Iskopaemye, 2014, No. 6, pp. 463–492.

Specific Features of the Distribution of Trace and Rare Earth Elements in Recent Bottom Sediments in the Lower Course of the Severnaya Dvina River and White Sea

A. V. Maslov[a], V. P. Shevchenko[b], V. N. Podkovyrov[c], Yu. L. Ronkin[a], O. P. Lepikhina[a], A. N. Novigatsky[b], A. S. Filippov[b], and N. V. Shevchenko[d]

[a]*Zavaritskii Institute of Geology and Geochemistry, Ural Branch, Russian Academy of Sciences, Pochtovyi per., 7, Yekaterinburg, 620075, Russia*
e-mail: maslov@igg.uran.ru

[b]*Shirshov Institute of Oceanology, Russian Academy of Sciences, Nakhimovskii pr. 36, Moscow, 117997 Russia*
e-mail: vshevch@ocean.ru

[c]*Institute of Precambrian Geology and Geochronology, Russian Academy of Sciences, nab. Makarova 2, St. Petersburg, 199034 Russia*
e-mail: vpodk@mail.ru

[d]*Moscow State University, Faculty of Geography, Leninskie gory 1, Moscow, 119991 Russia*
e-mail: snatti@yandex.ru

Received July 23, 2012

Abstract—The paper discusses results of the lithogeochemical examination of recent bottom sediments in the lower course of the Severnaya Dvina River and White Sea. It has been established that the average concentration of several trace elements (Hf, Sc, Co, Y, Ni, V, Cr, Zr, Ba, and others) therein correlates with the content of the silt–pelite fraction. Maximal concentrations of the majority of above elements are confined to the silty–clayey sediments at the Basin/Dvina Bay boundary. They localized near the coastal zone only for some clastophile (Zr, Cr, and others). Typical values of the hydrolyzate module, chemical index of alteration, and Al_2O_3/SiO_2 ratio in the aleuropelitic and pelitic sediments of the Severnaya Dvina River delta, Dvina Bay, and the Dvina Bay Basin boundary suggest that these sediments are confined to sufficiently cold climate settings. Data points of sediment composition in discriminant paleotectonic diagrams are scattered over a large field probably due to high contents of the weakly weathered plagioclases, micas, and amphiboles, as well as the hydrogenic process promoting the accumulation of Fe and Mn. The PAAS-normalized spectra of rare earth elements (REE) in bottom sediments of the Pinega and Severnaya Dvina rivers, marginal filter of the latter river, Dvina Bay, and the Dvina Bay Basin boundary are similar to the REE distribution in clayey rocks of the ancient platform cover (except for a slight positive Eu anomaly). The REE systematics and distribution pattern of compositional data points of recent bottom sediments in the Gd_N/Yb_N–Eu/Eu* and Eu/Eu*–Cr/Th diagrams and values of several indicator ratios of trace elements suggest that the studied rocks were formed by the mixing of clastic materials from geochemically contrast provenances: northwestern provenance (Kola–Karelia geoblock), which is mostly composed of the Archean and Early Proterozoic crystalline complexes, and the southeastern provenance (northwestern periphery of the Mezen syncline), which is almost totally composed of Phanerozoic sedimentary rocks. The latter provenance likely played a crucial role in the geochemical signature of recent bottom sediments over a significant area of the White Sea.

DOI: 10.1134/S0024490214060078

Lately, attention of researchers is being increasingly focused on peculiarities of the formation of recent bottom sediments in the White Sea along with its big and small rivers. This was stimulated appreciably by multidisciplinary investigations under the *White Sea System* program (Lisitsyn, 2010; Lisitsyn et al., 2010; *Sistema* ..., 2010). Owing to a complex geological history and structure, as well as diversity of natural processes, the White Sea has been considered for many years a "natural laboratory" (Nevesskii et al., 1977). The modern geological literature provides data on the contents of many elements, such as Fe, Mn, Al, Ti, P, S, and Ca, in recent sediments of the White Sea (Koukina et al., 2003; Peresypkin et al., 2004; Demina et al., 2005; Strekopytov et al., 2005; Rozanov et al., 2006). Our task was to analyze peculiarities of the distribution of a wide range of minor and trace elements (Li, Be, Na, Mg, Al, P, K, Ca, Sc, Ti, V, Cr, Mn, Fe, Co, Ni, Cu, Zn, Ga, Ge, As, Rb, Sr, Y, Zr, Nb, Mo, Ag, Cd, In, Sn, Sb, Te, I, Cs, Ba, Hf, Ta, W, Re, Au, Hg, TI, Pb, Bi, Th, and U), rare earth elements (REE), and platinum group elements (PGE) in recent bottom sediments of the White Sea and lower course of the Severnaya Dvina River. The first results obtained in this field are reported in (Maslov et al., 2012a). The present communication updates significantly the previous data. These works represent a contribution to *building a bridge* between our knowledge about recent sedimentogenesis and reconstruction of the geological past based on the relative lithological principle (Yapaskurt, 2010).

The periphery of continents has accumulated more than 90% of terrigenous material transported into marine basins and ocean (Lisitsyn, 1978). Data on the compositional transformation of this material, first of all REE and several other trace elements, relative to provenance rocks are lacking in the literature (Taylor and McLennan, 1985; Rollinson, 1994; *Geochemistry* ..., 2003; and others). The REE composition in clayey sediments of the continental periphery is similar to that in platform shales, such as North American Shale Composite (NASC), Post-Archean Australian Shale (PAAS), and others, although they are slightly depleted in HREE (Taylor and McLennan, 1985). The Ce anomaly is missing. In the deeper water and offshore (pelagic) sediments, the terrigenic material gives way to the hydrogenic variety. Pelagic sediments are commonly characterized by the accumulation of LREE and positive Ce anomaly (Dubinin, 2006) because of the sorbtion of REE dissolved in ocean water by the suspended material (primarily, ferromanganese oxyhydroxides). In contrast, metalliferous sediments of the pelagic zone show prominent negative Ce and positive Eu anomaly accompanied by a slight deficiency of LREE (Dubinin, 2006).

Study of the distribution of Fe, Mn, and Ti by Nevesskii et al. (1977) revealed that maximal contents of the above elements are confined to the deepest parts of the White Sea dominated by the fine-grained alumosiliciclastic sediments. This feature is also typical of estuarine zones of the Vyga and Onega rivers along with the Dvina Bay. In the latter case, however, this feature is related to the presence of Fe–Mn macro- and micronodules in the surface layer. Strekopytov et al. (2005) established that Fe–Mn formations in the Kandalaksha Bay lack anomalous REE concentrations relative to the host sediments. The typical negative Ce anomaly in the sediments suggests a hydrogenic source of REE. Rozanov et al. (2006) concluded that the distribution of Fe and Mn along the Kandalaksha–Arkhangel'sk profile shows a distinct asymmetry (maximal Mn concentrations are typical of sediments in the Kandalaksha Bay, while high Fe concentrations are confined to sediments of the White Sea Basin). According to these authors, such asymmetry is related to the rock composition in the provenance, as well as the hydrodynamic setting, seafloor morphology, and early diagenetic processes. According to Kuz'mina et al. (2009), Mn can be trapped both in the Kandalaksha Bay and the central White Sea Basin.

The composition and geochemistry of recent bottom sediments in the White Sea are controlled generally by two large provenances: Kola–Karelia geoblock (western and northwestern parts of the drainage area) and northwestern periphery of the Mezen syncline of the Russian Plate (southeastern White Sea region and its southern and southeastern sides) (Fig. 1) (Nevesskii et al., 1977; Lisitsyn, 2010; Gubaidullin, 2010). Approximately 85% of the first provenance is composed of tonalite–trondhjemite gneisses, granites, migmatites, granulites, tholeitic and ferrometabasalts, metadacites, metarhyolites, conglomerates, gabbro anorthosites, and alkali granites of the Archean age. The Lower Proterozoic rocks (diverse terrigenic and carbonate rocks, metapyroxenites, granophyres, and gabbroids) make up 10% of the Kola–Karelia geoblock area, whereas the Riphean sedimentary and igneous complexes make up no more than 5% of the region (*Dokembriiskaya* ..., 1988; *Geologicheskaya* ..., 1996a; *Rannii* ..., 2005).

The central and southern parts of the above structure comprise rocks of the Kola microcontinent (Mints et al., 2010). The microcontinent includes the Central Kola granulite–gneiss belt, Keivy volcanotectonic paleodepression, and Inari-Kola granite–greenstone zone, the eastern part of which includes the granite–greenstone complexes making up the Inari, Tersky, and Strel'na (Tersky–Strel'na) blocks (*Rannii* ..., 2005; Mints et al., 2010). The Tersky block is composed of granite gneisses (biotite, amphibole–biotite, amphibole, and other varieties mainly represented by metadacites), granodiorites, tonalites, and plagiogranites of the Tersky intrusive complex, and supracrustal rocks of the Sergov Sequence. The latter sequence includes the amphibole–biotite, garnet–amphibole–biotite gneisses, and amphibolites. Mica and garnet–mica gneisses are subordinate. Sedimentary protoliths of these rocks are mainly represented by graywackes; igneous protoliths, by basalts, basaltic andesites, andesites, and dacites (*Rannii* ..., 2005; and others). The Nd model age of granitoids of the Tersky Complex is 2.95–3.04 Ga (Daly et al., 2001). Metavolcanic rocks of the Sergov Sequence are dated at 2.22 and 2.16 Ga; metagraywackes, at 2.23 Ga (Daly et al., 2001). The southeastern Strel'na block includes granite gneisses resembling counterparts in the Tersky block (Belyaev, 1980; *Geologicheskaya* ..., 1996b). Their Nd model age is ~2.83 Ga (Timmerman and Daly, 1995). The western part of this block in the Varzuga River basin is composed of metasedimentary rocks of the Peschanoe Ozero Sequence (*Geologicheskaya* ..., 1996b) with the Nd model age of 2.69 Ga (Daly et al., 2001). As metagraywackes of the Sergov Sequence, biotite gneisses (metagraywackes) in the upper

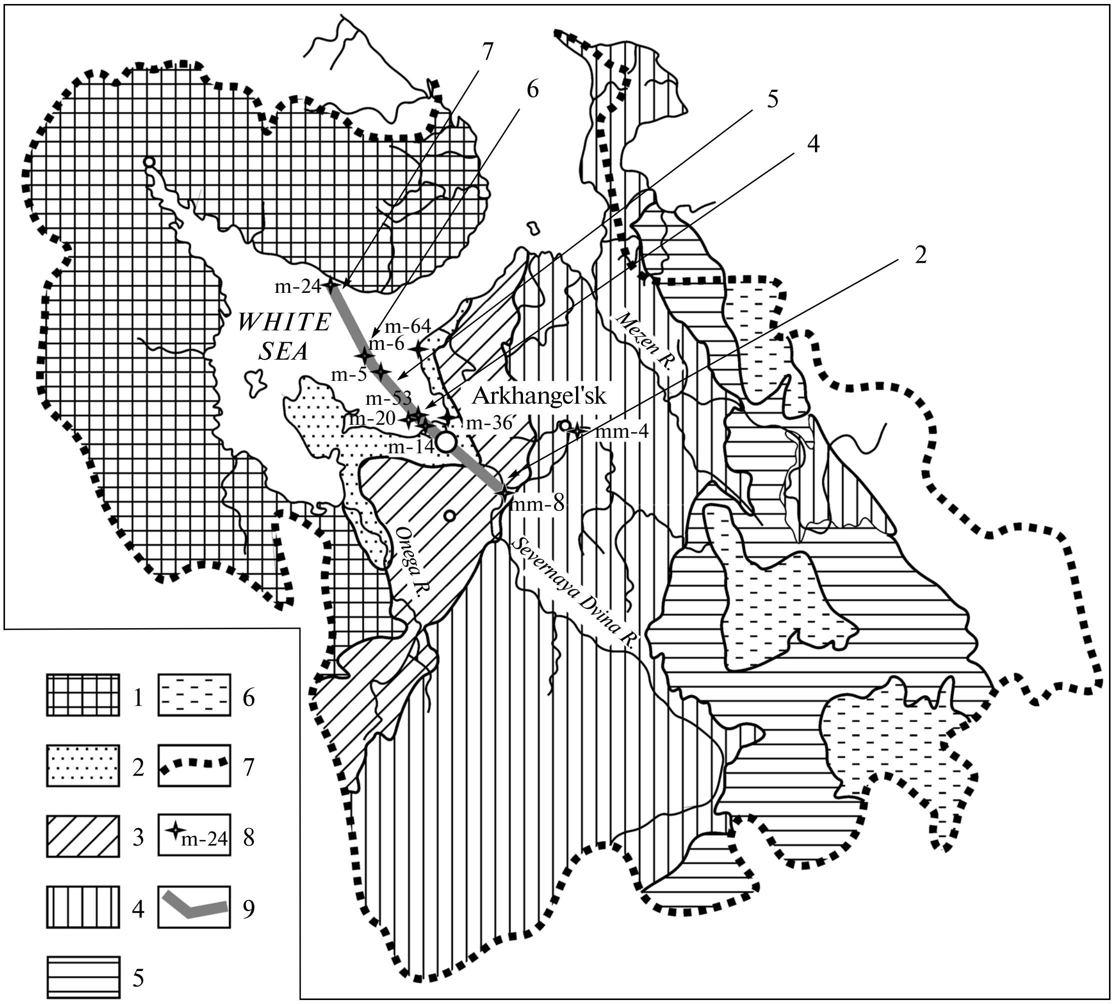

Fig. 1. Schematic geological structure of the catchment basin in the White Sea and location of samples examined for the Sm–Nd systematics. The catchment area is adopted from (Lisitsyn, 2010).(1–6) Age of rocks: (1) Archean and Proterozoic, (2) Vendian, (3) Carboniferous, (4) Permian, (5) Triassic, (6) Jurassic; (7) catchment boundary; (8) sample and number; (9) profile extending from the lower course of the Severnaya Dvina River to the Tersky coast of the Kola Peninsula; areas: (2) Pinega River area from the Pinega Settlement to the river mouth; (4) Severnaya Dvina River delta; (5) Dvina Bay; (6) Dvina Bay Basin boundary; (7) Tersky coast at the Varzuga River mouth.

course of the Strel'na River are characterized by the Nd model age of ~2.22 Ga (Timmerman and Daly, 1995).

The catchment area drained by the Severnaya Dvina and Onega rivers and their tributaries are composed of tuffogenic-terrigenic sediments of the Upper Vendian (Valdai Group), Paleozoic (Carboniferous and Permian), and Mesozoic (Gubaidullin, 2010). Upper Vendian rocks represented by the Lyamtsa, Verkhovka, Zimnie Gory, and Erga formations (Grazhdankin, 2003) are exposed on cliffs of the White Sea coast, along rivers cutting deep valleys in the White Sea–Kuloi plateau, as well as along the coast of the Dvina and Onega bays. Contents of many trace elements in the fine-grained clastic rocks of this area were determined in our previous regional lithogeochemical works (Maslov et al., 2008a, 2008b, 2009). Their UCC-normalized (Rudnick and Gao, 2003) values made it possible to determine Clarke concentrations (C_C)[1] and compare the latter parameter with C_C values of the above-mentioned trace elements in recent bottom sediments from different areas of the White Sea and basin of the lower course of the Severnaya Dvina River (hereafter, lower Severnaya Dvina basin). In Upper Vendian mudstones and clays, only Rb and Yb show median C_C values more than 1.50. Median C_C values are less than 0.70 for Cu, Sr, Mo, Ba, and Pb; for the remaining trace elements mentioned above, the median Clarke concentration ranges from 0.76 to 1.46

[1] According to V.I. Vernadsky, ratio of contents of the chemical element in a certain geochemical system and the Earth's crust is defined as Clarke concentration (Perel'man, 1979). Application of this parameter (C_C) provides insight into both individual and general geochemical features of various sedimentary rocks (Maslov et al., 2010b).

(Fig. 2a). At the same time, maximal C_C values do not exceed 1.50 for V, Co, Cu, Y, Zr, Nb, Mo, Cs, La, Ce, Nd, Sm, Eu, Gd, Hf, Ta, Pb, Bi, Th, and U.

As described in (Maslov et al., 2008b; Grazhdankin et al., 2010), the REE systematics in Upper Vendian and Cambrian rocks (Padun Formation) can be compared with the systematics in igneous rocks of mostly felsic composition: if the values are PAAS-normalized (Taylor and McLennan, 1985), the $(La/Yb)_{PAAS}$ value ranges from 0.6 to 1.4, parameter $(Gd/Yb)_{PAAS}$ variation range is 0.8–1.9, and the Eu anomaly[2] is positive (1.2). The Nd model age[3] of mudstones of the Upper Vendian Lyamtsa, Verkhovka, Zimnie Gory, and Erga formations varies from 1.73–1.71 to 1.57–1.53 Ga. In mudstones of the Cambrian Padun Formation, this parameter is 1.66–1.64 Ga (Maslov et al., 2008a). Value of $\varepsilon_{Nd}(0)$[4] for Vendian clayey rocks of the White Sea–Kuloi plateau varies from –11.1 to –19.2. As data on contents and ratios of trace elements, information about the REE systematics and $\varepsilon_{Nd}(0)$ and $t_{Nd}(DM)$ values therein are missing for the younger rocks in the southeastern provenance. Therefore, all further comparisons are based on the materials presented above.

MATERIAL AND METHODS

To examine regularities in the distribution of trace elements in recent bottom sediments of the White Sea and its southeastern provenance, we used a collection of more than 70 samples of the surface (0–3 cm) bottom sediments recovered by grabs in 2004–2006 during expeditions in the basin of the Severnaya Dvina River and its tributaries, as well as during cruises 49 and 55 of R/V *Professor Shtokman*. The grain size composition of bottom sediments was analyzed at the Shirshov Institute of Oceanology according to the routine procedure (Petelin, 1967).

Contents of trace elements and REE were determined at the Institute of Geology and Geochemistry (Ural Branch, Russian Academy of Sciences) with the high-resolution (HR) inductively coupled plasma sector field (SF) mass spectrometer (HR-ICP-MS ELEMENT 2) designed for the element and isotope analysis. The method was modified as compared to the version described in (Maslov et al., 2004a, 2004b). The starting material (50 mg of thoroughly ground powder) was decomposed in a hydrofluoric and nitric acid (5 : 1) mixture at 140–180°C in teflon autoclaves for 24–48 h depending on the sample composition. After evaporation to dryness, the study samples were treated in 6.2 N HCl and slowly distilled. Then, the obtained chlorides were treated with concentrated HNO_3 until the aqua regia formation. The cooled sample was treated in 1 mL of concentrated HNO_3, evaporated to dryness, and converted into 3% nitric acid solution with a starting sample dilution coefficient of about 10^3. The obtained solution was analyzed with HR-ICP-MS ELEMENT-2. To calibrate the mass spectrometer before the analysis of each sample series, we carried out measurements in solutions attested for the contents of elements under consideration. After each eight measurements, we checked the blank sample represented by the Basalt Columbia River Standard (BCR-2, US Geological Survey). To obtain the blank sample solution, we applied the sample preparation procedure similar to that used for decomposing the study samples. Most elements were determined under standard low resolution (R = 300) conditions. Contents of Fe, Cr, V, and As were measured under medium and high resolution (R = 4000 and 7000) conditions. Coefficient of variation in analysis reproducibility varied from 3 to 40% depending on element concentration in the starting sample.

Concentrations of Sm and Nd and their isotopic compositions were determined by the isotope dilution mass spectrometry (MS-ID). Chemical preparation of samples included the following procedures: (1) sample decomposition; (2) extraction of the total REE; and (3) fractionation of Sm and Nd. Samples were decomposed in the hydrofluoric and nitric acid mixture in teflon autoclaves. The weighed portion with a calculated amount of the mixed (^{150}Sm + ^{149}Nd) tracer (based on the optimal tracer/sample ratio) was kept at 130–180°C until complete decomposition. The reaction mixture was evaporated to dryness. Then, 10 N HCl was added for the breakdown of fluorides. The samples were kept at 110–130°C for 6 h and again evaporated. The dry residue was dissolved in 2 mL of 2.3 N HCl and centrifuged. The obtained solution was introduced into the first chromatographic column with an AG 50 (8200–400 mesh) cationite. In this column, the total REE was fractionated from the major components of sample by the stepwise (2.3 N and 3.9 N) HCl elution. Then, the eluate fraction containing Nd, Sm, and other REEs were evaporated and dissolved in 0.5 mL of 0.1 N HCl. The final fractionation of Sm and Nd was accomplished in the second chromatographic column by the extraction chromatography with a 2-ethylhexyl orthophosphoric acid coating on the polytrifluorochloroethylene (KEL-F). Elution was carried out with 0.3 N HCl (Nd) and 0.7 N HCl (Sm). All chemical operations were accomplished in a clean room with the forced supply of filtered atmo-

[2] The Eu anomaly (Eu/Eu*) is a chondrite-normalized parameter of REE distribution in rocks calculated according to the following formula: $(Eu_{sample}/Eu_{chondrite})/\sqrt{(Sm_{sample}/Sm_{chondrite}) \times (Gd_{sample}/Gd_{chondrite})}$.

[3] According to axiomatics of the Sm–Nd isotope geology accepted at present, the term *Nd model age* reflects the average model (not stratigraphic!) age of rocks, whose decay in provenances promoted the formation of various sedimentary rocks.

[4] $\varepsilon_{Nd}(0)$ is a dimensionless $10^4 \times [(^{143}Nd/^{144}Nd_{meas}/^{143}Nd/^{144}Nd_{CHUR})$ value demonstrating variations of the present-day $^{143}Nd/^{144}Nd$ ratio in the study object relative to $^{143}Nd/^{144}Nd_{CHUR}$ = 0.512638 for the Chondritic Uniform Reservoir.

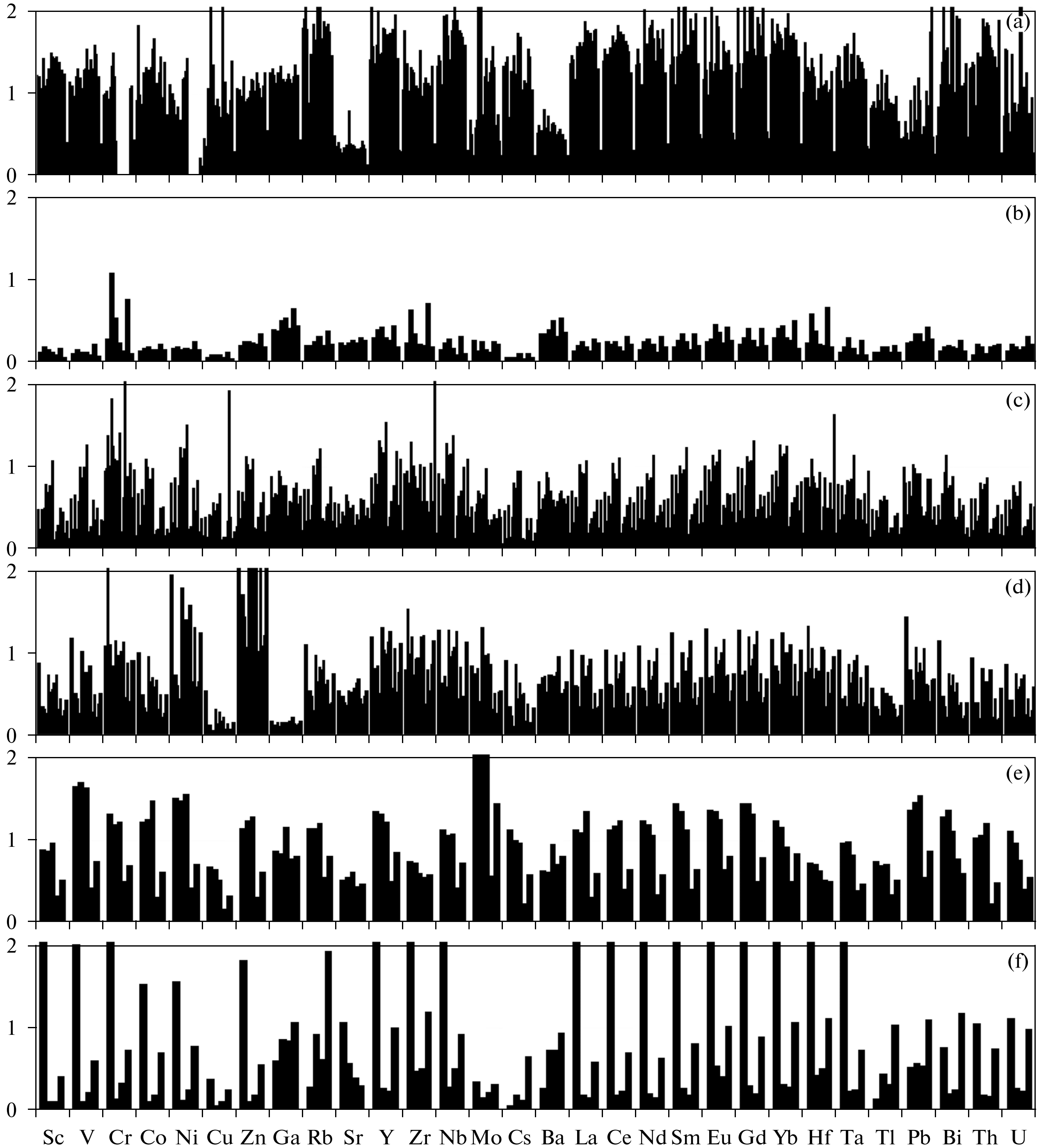

Fig. 2. The UCC-normalized contents of trace elements in the fine-grained clastic rocks. (a) Upper Vendian rocks of the White Sea–Kuloi plateau; (b–f) recent bottom sediments: (b) lower course of the Pinega River, (c) Severnaya Dvina River delta, (d) Dvina Bay, (e) Dvina Bay Basin boundary, (f) littoral zone of the Tersky coast (the number of columns in the element cell corresponds to the number of studied samples).

spheric air by HEPA filters, teflon and quartz dishware, and specially purified reagents. The laboratory blank did not exceed 0.3 ng for Nd and 0.2 ng for Sm.

Isotopic compositions of Sm and Nd in the ^{150}Sm + ^{149}Nd spike mixture and corresponding samples were determined with a Finnigan MAT 262 multicollector (MC) thermoionization mass spectrometer (TIMS) in the static mode using the rhenium evaporator and ionizer bands calcined preliminarily in vacuum. Reproducibility of the mass-spectrometric analysis of ^{143}Nd/^{144}Nd was not higher than 0.003%. The presence of systematic error was checked by measurments

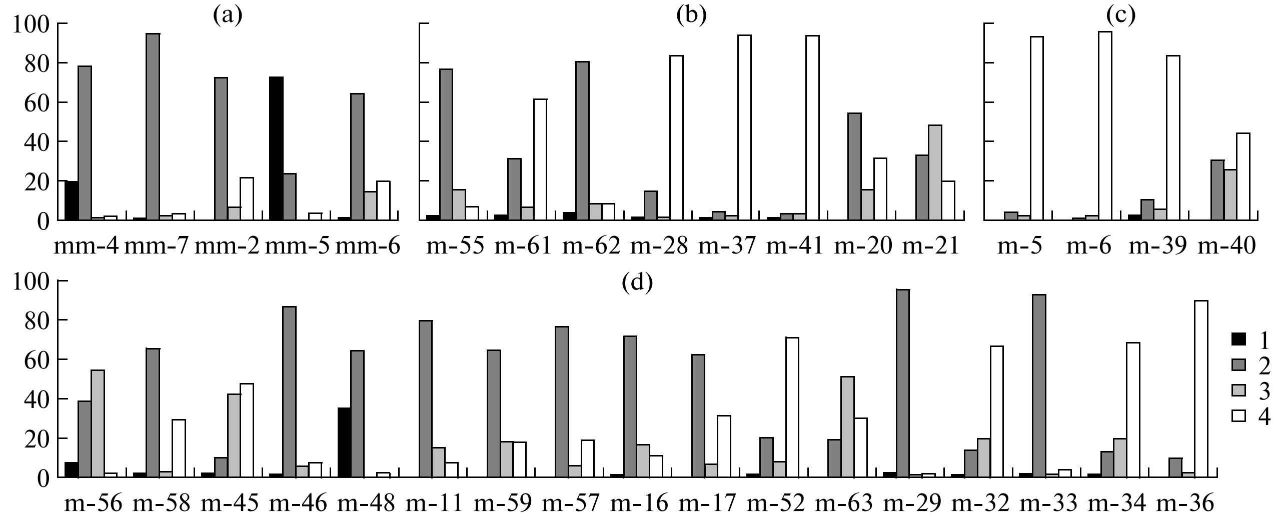

Fig. 3. Grain size composition of some representative samples of recent bottom sediments. (a) Lower course of the Pinega River; (b) Dvina Bay; (c) Tersky coast at the Varzuga River mouth; (d) Severnaya Dvina River delta. (1) gravel; (2) sand; (3) silt; (4) pelite.

of $^{143}Nd/^{144}Nd$ in the La Jolla standard. Reproducibility of measurment of $^{147}Sm/^{144}Nd$ (lower than 0.5%) was calculated by parallel measurements in BCR-2. Calculation and assessment of parameters in evolution diagrams were accomplished using the Isoplot/Ex ver. 3.6 software package (Ludwig, 2008).

To facilitate the perception of material during its further presentation and discussion of analytical data, we present overviews for several areas located along the virtual SE- to NW-oriented profile extending from the lower course of the Severnaya Dvina River to the Tersky coast of the Kola Peninsula: (1) Severnaya Dvina River section 20 km above the Pinega River inflow (1 sample); (2) Pinega River section extending from the Pinega Settlement to the rivermouth (7 samples); (3) Severnaya Dvina River section 2 km below the Pinega River inflow (1 sample); (4) Severnaya Dvina River delta (34 samples); (5) Dvina Bay (15 samples); (6) Dvina Bay Basin boundary (5 samples); and (7) Tersky coast at the Varzuga River mouth (4 samples). For 9 samples representing each of the areas mentioned above, we also determined $\varepsilon_{Nd}(0)$ values. In addition, we adopted data on the chemical composition of the surface layer of bottom sediments in the White Sea (Kuz'mina et al., 2009) for presentation of the overview of study areas and several genetic conclusions.

CHEMICAL COMPOSITION OF RECENT BOTTOM SEDIMENTS IN THE WHITE SEA

Approximately 40% of the studied samples belong to aleuropelites, sand make up about 54%, and silts account for 6%. The grain size composition of several representative samples taken from different parts of the study region is shown in Fig. 3. According to (Nevesskii et al., 1977), the pelite fraction of White Sea sediments comprises smectites and hydromicas (predominant), kaolinite, chlorite, and mixed-layer minerals. The content of smectites is maximal in the White Sea Basin and decreases appreciably toward the coasts. Absolute contents of smectites are very low in sediments of the Severnaya Dvina River delta. Absolute contents of hydromicas are also insignificant in sediments of large shallow-water zones and along coasts of the White Sea. In contrast, their contents increase to 10–25% in the silty and silty–pelitic sediments on slopes of the White Sea Basin and reach 25–50% or more in depressions in the central marine part.

Information about the content and distribution of Fe, Mn, Al, Ti, P, S, and Ca in recent sediments of the White Sea and Kandalaksha Bay is presented in (Nevesskii et al., 1977; Peresypkin et al., 2004; Strekopytov et al., 2005; Rozanov et al., 2006). Table 1 in (Kuz'mina et al., 2009) presents data on the bulk chemical composition (SiO_2, Al_2O_3, Fe_2O_3, MgO, CaO, K_2O, TiO_2, and MnO contents determined by the VRA-30 XRF analysis) of surficial bottom sediments in the White Sea (53 sites) recovered during cruises 49 and 80 of R/V *Professor Shtokman*. These studies revealed that the sediments under consideration are compositionally similar to normal terrigenous clastic clayey sediments, but they are distinguished by significant variations in contents of the major oxides (SiO_2 47–84%), Al_2O_3 5–14%, Fe_2O_3 1–9%, MgO 1–4%, CaO and K_2O 1–3%, TiO_2 0.1–0.9%, and MnO 0.02–5% or more). Based on the multidimensional statistic analysis, Kuz'mina et al. (2009) demonstrated that in terms of the chemical and grain size composition, recent sediments belong to the series of more or less uniform groups marked by certain zonal distribution on the White Sea bottom. For

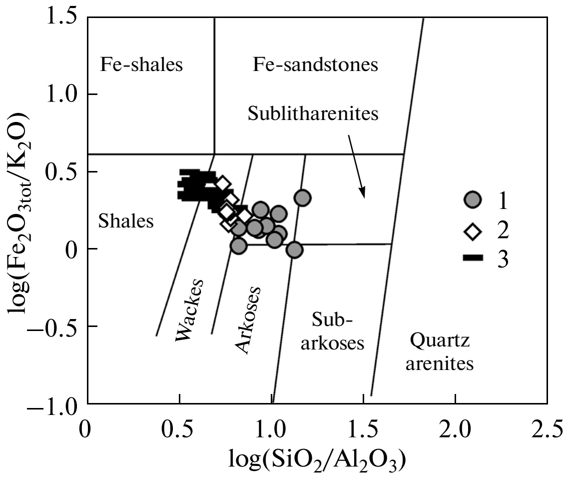

Fig. 4. Positions of data points of recent bottom sediments in the White Sea (Kuz'mina et al., 2009) in the $\log(Fe_2O_{3tot}/K_2O)$–$\log(SiO_2/Al_2O_3)$ diagram (Herron, 1988). (1) Sand; (2) silt; (3) aleuropelitic and pelitic sediment.

example, the Dvina Bay bottom is virtually covered with the fine-grained sand. Aleuropelitic sediments occur at the Dvina Bay Basin boundary and give way gradually to pelitic sediments downward the slope. These data support the concept of Nevesskii et al. (1977).

We adopted the data in (Kuz'mina et al., 2009) concerning the composition of surficial bottom sediments in the White Sea to compile $\log(Fe_2O_{3tot}/K_2O)$–$\log(SiO_2/Al_2O_3)$ diagram (Herron, 1988)[5]. As the $\log(Na_2O/K_2O)$–$\log(SiO_2/Al_2O_3)$ diagram (Pettijohn et al., 1973) and several discriminant paleotectonic diagrams, the diagram mentioned above makes it possible to classify sandstones and clayey rocks based on their chemical composition.

In the Herron's diagram, compositional data points of recent sandy sediments in the White Sea mainly cluster in the litharenite domain (Fig. 4). Data points of aleuropelitic sediments with a variable admixture of sand mainly plot in the wacke domain, whereas data points of the aleuropelitic and pelitic sediments[6] plot in the transitional zone between wackes and shales, supporting our earlier conclusion about similarity of the chemical composition of recent bottom sediments in the White Sea with that of "normal" terrigenous sediments (Kuz'mina et al., 2009).

[5] It is assumed that the Herron's diagram provides a more precise classification of arkoses and evaluation of the share of the less weathering-resistant Fe–Mg minerals in the rocks (Maslov, 2005). Two fields in the given diagram belong to clayey rocks usually marked by low SiO_2/Al_2O_3 values.

[6] We recalculated the contents of major oxides in the aleuropelitic and pelitic sediments reported in (Kuz'mina et al., 2009) to minimize the role of iron hydroxide microconcretions and nodules.

Distribution of Trace Elements

Contents of a wide range of trace elements in the representative samples of recent bottom sediments recovered from sites 3–6 are given in Table 1. Table 2 summarizes information pertaining to the median[7], minimal, and maximal contents of the trace elements and their indicator ratios in the studied samples. These parameters were used to compile various geochemical diagrams. Analysis of these data suggests the following conclusions.

In contrast to the upper continental crust (Rudnick and Gao, 2003), median C_C values for trace elements is significantly lower than 1 in all samples of recent bottom sediments from the lower course of the Pinega River (Fig. 2b). Maximal median value of C_C (0.43) is typical for Ga; minimal (0.05), for Cs. In the whole sampling, the maximal C_C value (1.08) is recorded for Cr. Such distribution of trace elements is likely related to predomination of the silt–sand fraction in the studied samples. As is known from (Taylor and McLennan, 1985; Cullers, 1995), this fraction is not the main concentrator of trace elements in sediments.

Approximately similar situation is also characteristic of bottom sediments in the Severnaya Dvina River delta (Fig. 2c). Here, the median C_C value is 0.91 only for Cr. Minimal median value is recorded for Cs (0.15); maximal value (given that Cr is not taken into consideration), for Zr (0.65). Maximal C_C values are also typical of Cr and Zr (2.73 and 2.05, respectively). For Ni, Cu, Y and Hf, these values range from 1.52 to 1.94.

For Sc, V, Co, Cu, Ga, Rb, Sr, Cs, Ba, La, Ce, Nd, Sm, Ta, Tl, Pb, Bi, Th, and U in samples of recent bottom sediments from the Dvina Bay, median C_C values do not exceed 0.70 × UCC (Fig. 2d). For Cr, Ni, Y, Zr, Nb, Mo, Eu, Gd, Yb, and Hf, they vary from 0.73 (Eu) to 1.14 (Ni). Clarke concentration of Zn here is much higher (2.17). Maximal C_C values are characteristic for Cr, Ni, Zn, and Zr (from 1.55 to 3.74 × UCC). For the remaining trace elements, they vary from 0.22 to 1.45.

In bottom sediments taken at the Dvina Bay Basin boundary, trace elements, such as V and Mo, are marked by median C_C values (more than 1.5); Cu, Sr, Zr, and Hf, by low values (less than 0.7). Maximal C_C values (more than 1.5) are typical for V, Ni, Mo, and Pb (Fig. 2e).

Finally, sediments from the littoral zone of the Tersky coast (mainly small- and fine-grained sand and aleurite) are marked by significant variations of C_C in the majority of analyzed trace elements (Fig. 2f). For example, maximal C_C value for Sc is 2.27 × UCC;

[7] In this paper, as in previous works, examination of limited (in volume) analytical samplings is based on the median contents and the ratios of various oxides and elements, because the given statistic parameter provides a generalized assessment of samplings with an unknown distribution pattern (Rock et al., 1987). Moreover "... application of median values is very convenient for the geochemical study of trace elements characterized by anomalous variability of contents." (Tkachev and Yudovich, 1975, p. 92).

Table 1. Contents of trace elements in representative samples of recent bottom sediments from different areas of the White Sea and lower course of the Severnaya Dvina River, ppm

Element	Area														
	1	2		3	4			5			6			7	
	Samples														
	mm-8	mm-2	mm-3	mm-1	m-27	m-34	m-63	m-15	m-38	m-65	m-5	m-22	m-40	m-23	m-24
Li	0.78	0.65	0.82	0.61	0.26	0.30	1.46	0.61	0.32	1.25	5.85	0.31	0.27	4.03	0.47
Be	0.36	0.38	0.39	0.40	1.80	1.87	0.69	0.37	1.96	0.67	1.62	1.94	1.68	2.32	0.87
Sc	4.42	1.97	0.78	1.39	3.47	12.22	4.63	3.29	7.25	4.06	12.48	13.48	7.15	31.71	1.42
V	21.77	11.29	6.80	10.79	29.67	118.60	32.79	23.26	55.79	36.27	160.98	159.00	71.36	195.57	8.92
Cr	194.89	49.73	8.51	16.94	38.56	110.61	87.95	303.39	89.10	83.67	120.95	112.13	63.33	223.41	11.73
Mn	478.06	160.33	77.59	162.16	273.32	757.06	309.11	273.98	403.57	324.88	1962.69	9295.83	547.11	2390.48	81.80
Co	4.38	2.98	2.57	2.81	6.06	18.61	4.08	3.73	11.33	4.59	21.08	25.61	10.63	26.53	1.54
Ni	12.36	6.55	7.05	10.09	17.09	64.61	16.66	10.49	32.00	18.15	71.40	73.21	33.38	73.72	5.61
Cu	3.31	2.07	0.90	1.83	6.02	15.93	5.48	3.07	8.92	4.66	19.16	14.40	8.81	10.41	1.33
Zn	24.29	16.19	12.00	9.49	58.00	67.30	26.21	20.74	39.66	21.25	76.87	86.81	41.51	122.26	6.39
Ga	6.55	8.85	7.61	7.10	9.61	11.97	11.08	8.49	12.62	11.21	15.28	20.23	14.06	10.50	14.85
Ge	1.41	1.02	0.98	1.09	2.30	4.04	0.98	1.15	2.64	1.04	5.51	4.91	2.85	7.11	1.92
As	0.22	0.19	0.65	0.42	0.40	1.29	0.68	0.26	0.61	1.23	5.84	5.73	1.08	0.24	0.10
Rb	14.60	19.88	18.02	16.79	34.59	75.29	45.83	22.10	55.02	33.42	96.72	101.73	67.76	22.41	77.54
Sr	67.82	74.12	82.43	101.46	118.63	115.97	155.57	99.88	165.84	150.10	164.79	195.03	148.38	338.35	179.36
Y	12.86	8.88	3.66	4.51	10.21	25.66	22.81	12.06	21.70	16.10	28.40	25.83	18.00	66.16	5.33
Zr	102.53	67.41	34.30	27.00	152.75	134.09	395.47	298.89	182.73	165.99	144.67	113.65	112.57	999.44	89.63
Nb	4.30	3.33	1.26	1.60	6.82	15.55	13.00	5.59	11.47	5.69	13.51	13.01	8.75	119.45	3.26
Mo	0.16	0.26	0.24	0.18	0.72	0.73	0.40	0.22	0.82	0.57	3.31	7.78	1.60	0.37	0.16
Cd	0.13	0.10	0.05	0.05	0.37	0.33	0.29	0.22	0.36	0.17	0.30	0.34	0.27	1.03	0.13
Sn	0.48	0.38	0.23	0.25	1.07	2.87	1.23	0.71	1.58	0.98	2.44	2.54	1.63	7.71	0.54
Sb	0.07	0.07	0.04	0.05	0.16	0.29	0.15	0.08	0.21	0.14	0.71	0.72	0.23	0.07	0.03
Te	0.06	0.04	0.03	0.04	0.26	0.30	0.16	0.08	0.32	0.14	0.18	0.31	0.27	0.35	0.13
I	0.53	0.56	0.57	0.55	0.31	0.30	0.64	0.57	0.40	0.64	1.01	1.44	0.53	0.22	0.24
Cs	0.21	0.28	0.22	0.27	1.11	5.03	0.91	0.34	2.15	0.75	5.51	4.77	2.87	0.27	0.83

Table 1. (Contd.)

Element	Area														
	1	2		3	4			5			6			7	
	Samples														
	mm-8	mm-2	mm-3	mm-1	m-27	m-34	m-63	m-15	m-38	m-65	m-5	m-22	m-40	m-23	m-24
Ba	188.50	238.46	221.57	261.16	369.83	346.16	400.13	283.05	460.30	343.21	389.92	590.25	506.47	164.78	454.90
La	6.77	7.48	7.21	5.13	11.40	27.96	18.00	14.49	21.11	10.49	35.10	42.22	18.43	71.29	5.74
Ce	13.81	15.25	13.55	10.71	22.50	48.63	35.17	28.58	42.80	22.21	70.92	78.67	40.74	155.99	11.07
Pr	1.63	1.77	1.38	1.27	2.80	6.59	4.30	3.38	5.15	2.49	8.98	8.11	4.48	18.42	1.33
Nd	6.45	7.50	5.01	4.86	10.07	23.92	16.04	12.88	18.17	10.46	33.72	28.80	15.80	61.81	5.27
Sm	1.30	1.59	0.91	0.99	2.01	4.87	3.26	2.32	3.32	2.12	6.81	5.31	3.04	11.70	1.20
Eu	0.33	0.45	0.27	0.33	0.51	1.09	0.67	0.48	0.86	0.53	1.37	1.26	0.81	2.56	0.53
Gd	1.42	1.65	0.80	0.92	1.76	4.86	2.71	2.13	3.39	1.83	5.78	5.28	3.16	11.41	1.16
Tb	0.26	0.26	0.12	0.14	0.29	0.77	0.41	0.33	0.55	0.30	0.85	0.78	0.49	1.81	0.17
Dy	1.81	1.56	0.67	0.75	1.73	4.31	2.44	2.02	3.29	2.01	4.85	4.47	2.92	11.04	0.96
Ho	0.42	0.33	0.13	0.15	0.37	0.88	0.54	0.43	0.68	0.42	0.97	0.86	0.61	2.48	0.21
Er	1.30	0.89	0.37	0.39	1.07	2.39	1.52	1.30	2.03	1.22	2.71	2.23	1.72	7.13	0.58
Tm	0.22	0.13	0.05	0.06	0.17	0.36	0.24	0.21	0.32	0.19	0.40	0.31	0.27	1.19	0.09
Yb	1.41	0.86	0.34	0.37	1.13	2.36	1.63	1.40	2.01	1.30	2.48	1.85	1.68	8.43	0.61
Lu	0.23	0.13	0.05	0.06	0.19	0.39	0.28	0.24	0.32	0.21	0.38	0.27	0.26	1.37	0.10
Hf	2.54	1.95	0.92	0.78	4.21	3.69	8.69	7.03	4.16	4.23	3.81	3.30	2.68	24.25	2.23
Ta	0.32	0.27	0.07	0.09	0.38	0.89	0.84	0.35	0.57	0.35	0.87	0.74	0.43	8.82	0.20
W	0.17	0.17	0.07	0.10	0.32	0.87	0.64	0.18	0.60	0.30	1.07	1.11	0.49	0.64	0.09
Tl	0.12	0.16	0.10	0.11	0.27	0.60	0.22	0.15	0.39	0.21	0.67	0.64	0.46	0.11	0.39
Pb	5.62	5.89	4.75	4.90	13.23	15.15	8.57	6.34	12.91	11.34	23.28	26.31	14.70	8.82	9.70
Bi	0.06	0.03	0.02	0.02	0.09	0.15	0.04	0.03	0.10	0.04	0.21	0.18	0.10	0.12	0.03
Th	1.16	1.84	2.18	3.00	3.07	9.19	4.23	3.82	5.12	2.12	10.81	12.73	5.15	11.01	1.90
U	0.41	0.50	0.58	0.84	0.82	1.73	1.36	0.87	1.47	0.79	2.99	2.06	1.50	3.01	0.69

Table 2. Contents of some trace elements (ppm) and their indicator ratios in recent bottom sediments from different areas of the White Sea and lower course of the Severnaya Dvina River

Elements and ratios	Area				
	2	4	5	6	7
Sc	1.7 / 0.8–2.5	3.2 / 1.0–14.9	6.0 / 3.1–12.2	12.1 / 4.5–13.5	3.5 / 1.4–31.7
Ti	570.4 / 246.0–1423.1	1502.1 / 243.7–4586.5	2623.1 / 1029.7–4792.8	3413.4 / 1572.2–4081.6	2009.1 / 375.1–8672.9
Cr	21.2 / 8.5–99.6	36.0 / 6.2–251.3	78.9 / 37.8–303.4	78.3 / 45.9–120.9	28.9 / 11.7–223.4
Co	2.7 / 2.3–3.7	4.0 / 1.3–18.9	6.9 / 3.7–17.5	12.2 / 5.4–25.6	3.7 / 1.5–26.5
Y	6.2 / 3.7–9.2	10.3 / 4.2–32.3	20.9 / 10.5–27.5	25.8 / 10.7–28.4	13.2 / 4.9–66.2
Zr	44.9 / 34.3–139.2	112.8 / 28.7–395.5	179.7 / 72.6–298.9	113.7 / 104.3–144.7	163.4 / 89.6–999.4
Nb	2.0 / 1.1–3.8	4.6 / 0.9–16.6	9.9 / 5.2–15.5	12.7 / 5.0–13.5	8.5 / 3.3–119.5
Ba	221.6 / 194.5–331.3	359.4 / 191.4–581.0	429.5 / 283.1–598.7	441.1 / 378.2–590.2	455.2 / 164.8–581.1
La	5.7 / 4.0–8.7	8.8 / 4.0–33.1	16.2 / 9.6–32.2	20.7 / 9.5–42.2	8.4 / 4.3–71.3
Ce	13.0 / 8.3–19.7	18.0 / 8.0–69.2	33.8 / 20.1–65.7	47.8 / 25.1–78.7	20.9 / 11.1–156.0
Sm	1.1 / 0.7–1.6	1.9 / 0.7–5.8	3.0 / 1.7–5.9	5.3 / 1.9–6.8	2.5 / 0.8–11.7
Eu	0.3 / 0.2–0.5	0.5 / 0.2–1.2	0.7 / 0.4–1.3	1.3 / 0.6–1.4	0.8 / 0.4–2.6
Gd	1.1 / 0.7–1.7	1.7 / 0.7–5.3	3.0 / 1.6–5.2	5.3 / 2.0–5.8	2.4 / 0.8–11.4
Yb	0.6 / 0.3–1.0	1.0 / 0.4–2.5	1.7 / 1.0–2.5	1.9 / 1.0–2.5	1.4 / 0.6–8.4
Hf	1.4 / 0.9–3.5	1.9 / 0.8–8.7	4.0 / 1.8–7.0	3.2 / 2.7–3.8	3.8 / 2.2–24.2
Th	1.5 / 0.8–2.3	1.9 / 0.7–9.2	3.9 / 1.9–9.8	5.6 / 2.3–12.7	2.9 / 1.6–11.0
Cr/Th	12.2 / 3.9–43.5	18.2 / 6.9–112.6	17.3 / 10.2–79.4	11.5 / 8.8–20.0	10.5 / 6.2–20.3
La/Th	3.5 / 2.2–5.4	4.1 / 2.7–6.0	3.9 / 2.8–5.1	3.4 / 3.0–4.1	3.1 / 2.3–6.5
Ce/Cr	0.3 / 0.1–1.6	0.3 / 0.1–1.3	0.4 / 0.1–0.6	0.6 / 0.5–0.7	0.6 / 0.5(0.9)
Co/Hf	1.6 / 0.9–2.8	1.7 / 0.5–5.0	1.6 / 0.5–4.3	4.0 / 2.0–7.7	1.1 / 0.7–2.0

Table 2. (Contd.)

Elements and ratios	Area				
	2	4	5	6	7
La/Y	0.8 0.7–2.0	1.0 0.7–1.3	1.0 0.7–1.3	1.2 0.9–1.6	1.0 0.8–1.1
Sc/Cr	0.07 0.02–0.10	0.08 0.01–0.16	0.08 0.01–0.12	0.11 0.10–0.12	0.10 0.05–0.14
Zr/Sc	34.3 26.5–61.7	26.4 11.0–85.4	6.3 12.6–90.9	11.6 8.4–23.3	52.0 31.5–59.0
Th/Sc	0.9 0.5–2.8	0.7 0.4–1.3	0.8 0.5–1.2	0.87 0.51–0.94	1.2 0.3–1.3
Sc/Th	1.1 0.4–2.2	1.5 0.8–2.6	1.2 0.9–1.9	1.2 1.1–2.0	0.8 0.7–2.9
Ti/Nb	288.7 195.7–329.5	278.0 168.3–435.7	260.6 183.7–433.1	302.0 262.3–318.7	125.2 72.6–291.0
La/Sc	3.5 2.4–9.2	2.9 2.0–4.4	2.9 2.3–4.4	2.8 2.1–3.1	3.1 2.2–4.1
Th/Co	0.6 0.3–0.9	0.5 0.3–1.0	0.5 0.4–1.0	0.50 0.42–0.52	0.6 0.4–1.2
Ba/La	38.2 30.7–57.4	35.4 11.1–62.4	21.8 12.0–62.2	14.0 11.1–46.4	55.9 2.3–105.1
La/Yb	8.6 6.7–21.2	10.6 6.0–15.4	10.5 8.1–13.7	14.1 9.6–22.8	8.4 7.7–9.4
ΣREE	32.8 20.4–46.6	65.5 20.3–166.0	95.7 48.4–158.6	136.1 55.2–180.4	131.0 27.6–366.6
$(La/Yb)_{PAAS}$	0.6 0.4–0.6	0.7 0.4–1.1	0.8 0.5–1.0	1.1 0.4–1.8	0.6 0.5–0.7
$(La/Sm)_{PAAS}$	0.75 0.7–0.8	0.8 0.7–1.0	0.8 0.7–1.0	0.9 0.2–1.2	0.8 0.7–0.9
$(Gd/Yb)_{PAAS}$	0.95 0.8–1.1	1.0 0.7–1.3	1.1 0.8–1.4	1.4 0.2–1.7	0.9 0.8–1.1
$(Eu/Eu^*)_{PAAS}$	1.3 1.1–1.5	1.3 1.0–1.6	1.2 1.0–1.6	1.2 0.2–1.5	1.7 1.0–2.3
La_N/Yb_N	6.7 4.5–14.3	7.0 4.1–10.4	7.3 5.5–9.3	9.8 6.5–15.4	5.7 5.2–5.3
La_N/Sm_N	3.5 3.0–5.0	3.6 2.9–4.4	3.6 2.v–4.3	3.7 3.1–5.0	3.3 3.0–3.8
Gd_N/Yb_N	1.3 1.1–1.9	1.4 1.0–1.8	1.4 1.1–1.9	1.8 1.5–2.3	1.3 1.1–1.5
Eu/Eu*	0.9 0.7–1.0	0.8 0.7–1.1	0.8 0.7–1.0	0.8 0.7–1.0	1.0 0.7–1.5
Ce/Ce*	1.01 0.98–1.81	1.00 0.84–1.12	1.02 0.95–1.30	1.01 0.94–1.30	1.08 0.94–1.54
n	6	34	15	5	4

In the nominator, median value; in the denominator, minimal and maximal values. *n* is the number of analyzed samples.

minimal, $0.10 \times$ UCC. For Cr, Ni, Zn, Y, and La, these values are 2.43 and 0.13, 1.57 and 0.12, 1.82 and 0.10, 3.15 and 0.23, 2.30 and 0.14, respectively. At the same time, median C_C values do not exceed $0.70 \times$ UCC only for Ga, Rb, Zr, Nb, Ba, Eu, and Hf. Maximal C_C value (9.95, sample m-23) is typical of Nb.

Contents of Sc, Cr, and Co in sediments increase from the lower course of the Severnaya Dvina River to the Dvina Bay Basin boundary. At sites 4 and 7, standard deviations slightly exceed the median contents, testifying to the irregular distribution of trace elements in individual samples. This pattern is typical of both deltaic zone and littoral sediments of the Tersky coast, because the degree of clastic material mixing/homogenization is relatively low in both cases. For Cr, irregular distribution in samplings is recorded not only in two areas mentioned above, but also in the lower course of the Pinega River. In all of the studied samples, median Ba contents are higher than dispersion.

Maximal Ba_{median} value is recorded in recent bottom sediments of the Tersky coast; minimal values, in sediments of the Severnaya Dvina River sampled above the Pinega River mouth. Median Hf content increases from 1.2 ppm in sediments from the lower course of the Pinega River to 2.8 ppm in the Severnaya Dvina River delta. In sediments from the Dvina Bay and littoral zone of the Tersky coast, Hf_{median} values are maximal and virtually comparable (4.2 and 4.3 ppm, respectively) in all of the studied areas. However, the Tersky coast is characterized by a significant (more than one order of magnitude) scatter of minimal and maximal concentrations of this element (2.2 and 24.2 ppm, respectively). Almost similar pattern is also recorded in the distribution of median contents for Th.

Figure 5 shows correlation between the amount of the silt–pelite fraction in sediments versus average contents of Hf, Sc, Co, Y, Ni, V, Cr, Zr, and Ba (choice of precisely these elements was dictated by their application for compiling various diagrams discussed below) in different areas (2, 4–6). Maximums of the majority of above-mentioned elements correspond to sediments with the highest content of clay (site 6). In sediments of the Dvina Bay, the highest contents are typical only for Zr, Cr and Hf, whose concentration in sediments is primarily controlled by the amount of accessory minerals (Figs. 5b, 5c, 5d).

Distribution of REE

The average total REE content in the studied samples varies from 26–37 (Severnaya Dvina River sectors above and below the Pinega River mouth and lower course of the Pinega River) to 66–96 (Severnaya Dvina River delta and Dvina Bay) and approximately 130 ppm (Dvina Bay Basin boundary and Tersky coast of the Kola Peninsula). These values are slightly lower than in particulates from the Severnaya Dvina River reported in (Pokrovsky et al., 2010; Shevchenko et al., 2010), but the general pattern of REE distribution in sediments does not differ basically. Contents of La vary from 4.0 to 8.7 ppm in sediments from the lower course of the Severnaya Dvina and Pinega rivers; in sediments from the Dvina Bay and White Sea Basin, from 9.5 to 32 ppm (as much as 42 ppm in some places). In the littoral (weakly mixed or weakly homogenized) sediments of the Tersky coast, variations of La are as significant as for Ce, Hf, and Th (Table 2).

Content of the silt–pelite fraction in sediments shows direct correlation with the total REE and La_N/Yb_N (Figs. 6a, 6b). At the same time, Gd_N/Yb_N[8] shows a very weak correlation with the content of the fine fraction (Fig. 6c).

The PAAS-normalized REE distribution in bottom sediments of the Pinega River sampled from the Pinega Settlement to the river mouth characterized by rather low-angle slightly MREE-oriented shape (Fig. 7a) and the following peculiarities: $(La/Yb)_{PAAS} = 0.56 \pm 0.09$; $(La/Sm)_{PAAS} = 0.75 \pm 0.06$; HREE depletion is lacking: $(Gd/Yb)_{PAAS} = 0.95 \pm 0.13$; and Eu (relative to PAAS) anomaly varies from 1.08 to 1.52. These spectra are somewhat similar to the REE spectra of clayey rocks in the cover of ancient platforms, such as Russian, North American, and Chinese (Ronov and Migdisov, 1996), but they show a more distinct positive Eu anomaly.

Bottom sediments of the Severnaya Dvina River above and below the Pinega River mouth are marked by both lower and higher values of $(La/Yb)_{PAAS}$, $(Eu/Eu^*)_{PAAS}$, and other parameters (Fig. 7c, Table 2) probably suggesting the lack of efficient mixing of sediments in some places due to a relatively slow current and/or the influence of tributaries. At the same time, the REE distribution in bottom sediments of the Severnaya Dvina River delta does not differ virtually from that in sediments of the Pinega River (Fig. 7d), although the total REE content is slightly lower in the latter case. Except for a slightly lower medium $(Eu/Eu^*)_{PAAS}$ value, this pattern is also typical of recent bottom sediments in the Dvina Bay.

Recent bottom sediments in all of the areas mentioned above are characterized by a sufficiently distinct positive (relative to PAAS) Eu anomaly. Its value ranges from 1.1 to 1.3 and reaches ~1.6 in the sample taken from the Severnaya Dvina River 2 km below the Pinega River mouth. Almost similarly high medium $(Eu/Eu^*)_{PAAS}$ value (~1.68) is typical of samples taken in the littoral zone near the Tersky coast of the White Sea. Here, maximal value of this parameter is ~2.3 (sample m-25, Fig. 7e).

To compare with the above data, we accomplished the PAAS normalization of REE contents in the main

[8] La_N/Yb_N and Gd_N/Yb_N—parameters of the chondrite-normalized REE distribution in various rocks. They are calculated using the following formulas: $La_N/Yb_N = (La_{sample}/La_{chondrite})/(Yb_{sample}/Yb_{chondrite})$; $Gd_N/Yb_N = (Gd_{sample}/Gd_{chondrite})/(Yb_{sample}/Yb_{chondrite})$.

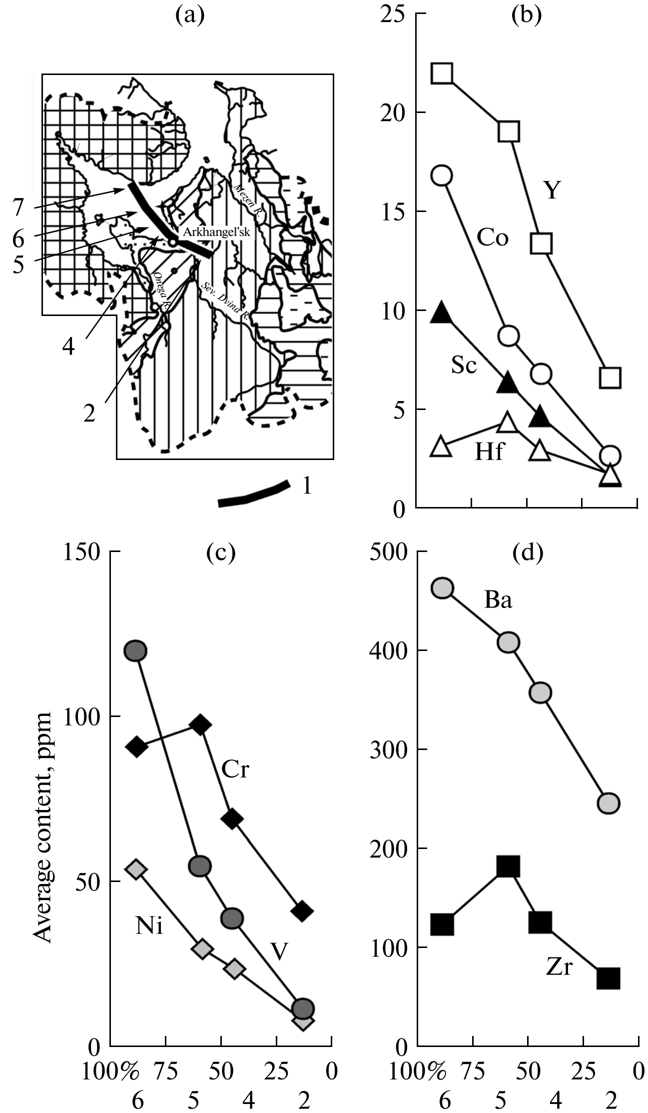

Fig. 5. Peculiarities of the profilewise variation in average contents of some minor and trace elements in recent bottom sediments from different areas of the White Sea and lower Severnaya Dvina basin in connection with the amount of the silt–pelite fraction in sediments. (a) Schematic position of the profile; (b–d) variation in contents of: (b) Y, Co, Sc, and Hf; (c) Cr, V, and Ni; (d) Ba and Zr. (1) Profile. Other symbols as in Fig. 1.

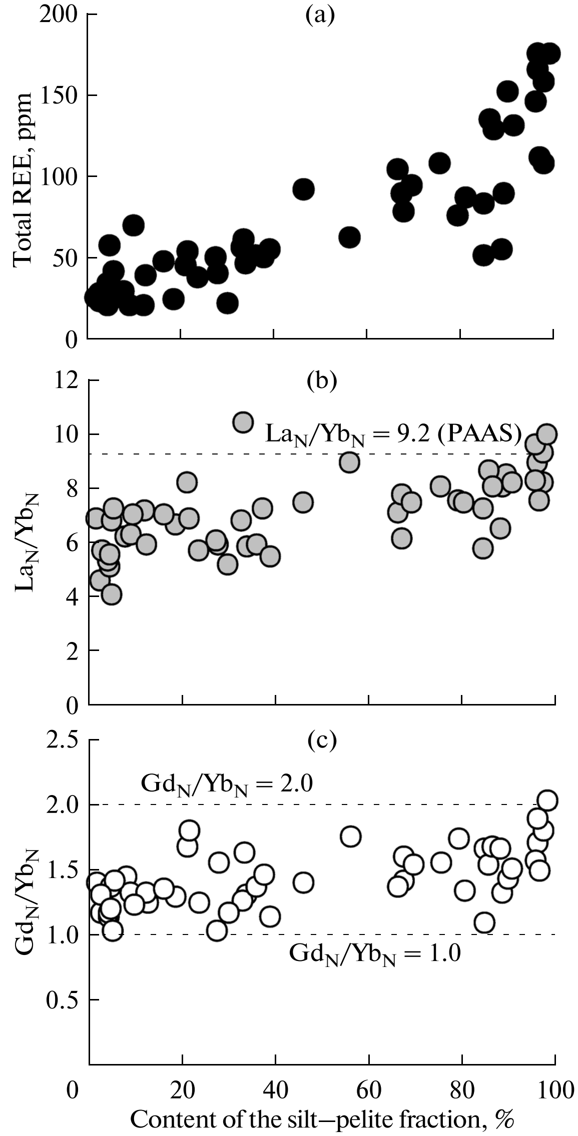

Fig. 6. Relationship between the silt–pelite fraction and geochemical parameters in recent bottom sediments of the White Sea and lower Severnaya Dvina basin: (a) total REE, (b) La_N/Yb_N, and (c) Gd_N/Yb_N.

types of igneous rocks of different ages ranging from Early Archean to Meso-Cenozoic (Condie, 1993). Based on the results of calculations, the medium $(La/Yb)_{PAAS}$ value for basalts is 0.29 ± 0.07 and medium $(Eu/Eu^*)_{PAAS}$ is 1.50 ± 0.13; i.e., basalts are marked by appreciable (relative to PAAS) depletion in REE and distinct positive Eu anomaly. For andesites, the parameters mentioned above are 0.75 ± 0.11 and 1.14 ± 0.11, respectively. Granites are characterized by a slight (relative to PAAS) enrichment in LREE—$(La/Yb)_{PAAS} = 1.26 \pm 0.51$—and distinct negative Eu anomaly—$(Eu/Eu^*)_{PAAS} = 0.60 \pm 0.12$. In felsic effusives, the $(La/Yb)_{PAAS}$ value is intermediate between that in basalts and andesites (0.65 ± 0.19), while the Eu anomaly (relative to PAAS) is positive but very low (1.10 ± 0.24).

The above data on the PAAS-normalized REE concentrations in the studied sediments certainly indicate that they represent sufficiently homogeneous (but not always well-mixed) fine-grained rocks. Even at the Dvina Bay Basin boundary, where the most elutriated and more or less well-mixed pelites should be present, two out of five samples of recent bottom sediments taken here (samples m-39 and m-40) are marked by significantly higher $(Eu/Eu^*)_{PAAS}$ values and, conversely, depleted (relative to the remaining

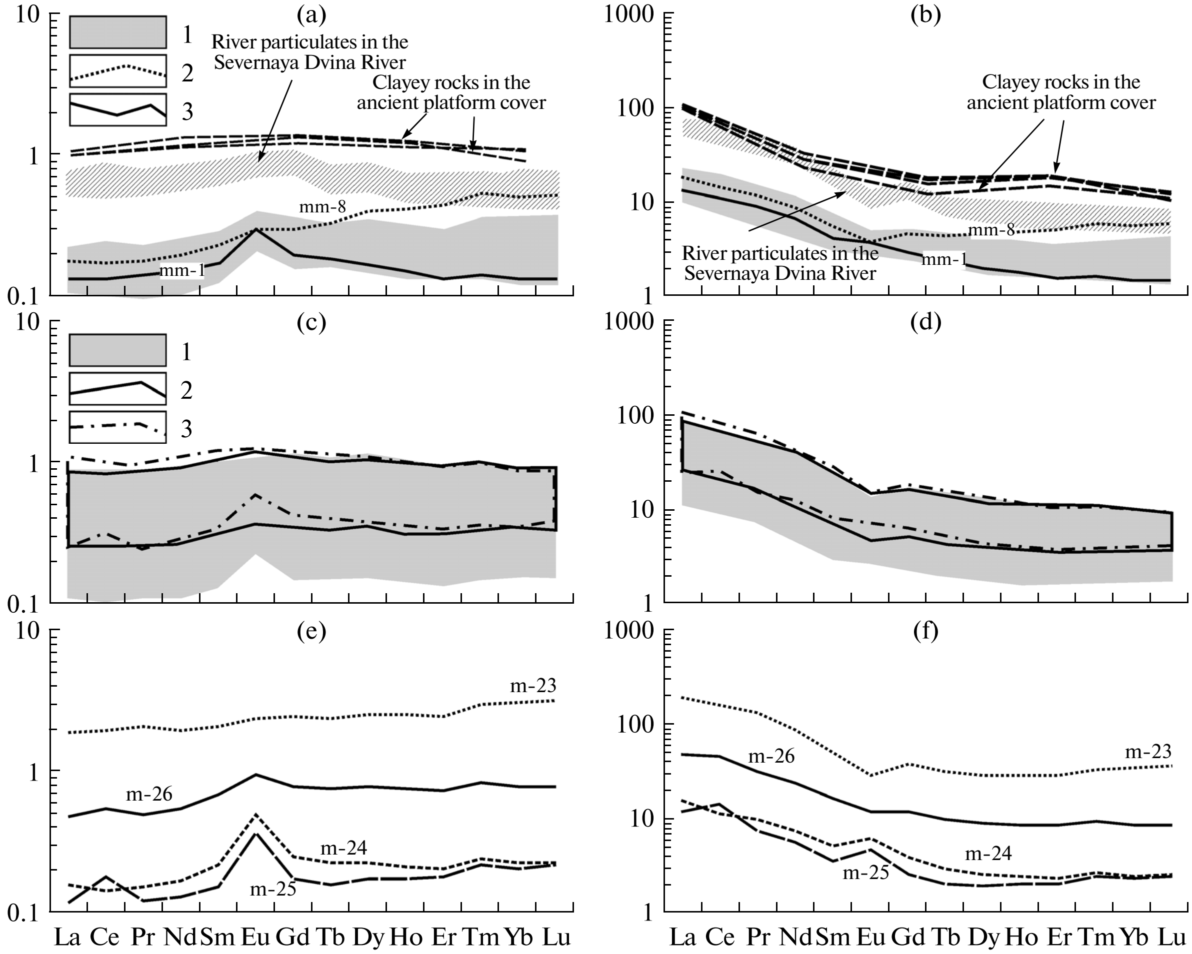

Fig. 7. The PAAS-normalized (a, c, e) and chondrite-normalized (b, d, f) spectra of REE distribution in recent bottom sediments of the White Sea and lower course of the Severnaya Dvina River. Samples in (a) and (b) were taken from: (1) lower course of the Pinega River extending from the Pinega Settlement to its inflow into the Severnaya Dvina River, (2) Severnaya Dvina River area 20 km above the Pinega River inflow, and (3) Severnaya Dvina River area 2 km below the Pinega River inflow. Samples in (c) and (d) were taken from: (1) Severnaya Dvina River delta, (2) Dvina Bay, and (3) Dvina Bay Basin boundary. Samples in (e) and (f) were taken from the Tersky coast of the Kola Peninsula at the Varzuga River mouth.

samples) $(La/Yb)_{PAAS}$ values. This observation is supported well by the composition of recent bottom sediments of the White Sea sampled during cruises 49 and 80 of R/V *Professor Shtokman* (Kuz'mina et al., 2009). For example, seafloor at site 6059 (depth 83 m) contains the pelitic–sandy–silty sediment with gravel and pebble; site 4697 (depth 87 m) includes the sandy–clayey silt with an admixture of pebble and gruss; and site 6061 (depth 118 m) includes the sandy–pelitic sediment with a minor admixture of pebble and rubble.

Correlation between Eu/Eu* and Ce/Ce* is absent or very weak in the most representative (in terms of the amount of recovered samples) sediments (sites 2, 4, and 5). In samples taken at the Dvina Bay/White Sea Basin boundary, correlation of these parameters is ~1.0. Positive correlation between Ce/Ce* and total REE is lacking for all sites mentioned above (Fig. 8). According to (Yan et al., 2012), this fact suggests that the REE distribution in sediments can be used for reconstructing the rock composition in catchment basins.

To provide insight into specific features of the REE distribution in recent bottom sediments of the White Sea and lower Severnaya Dvina basin, we also accomplished chondrite normalization (Taylor and McLennan, 1985) of the REE contents in samples. The results unraveled the following properties of bottom sediments from the lower course of the Pinega River: the median La_N/Yb_N value is 5.4, which is slightly higher than in recent sediments of the Severnaya Dvina River 20 km above the Pinega River inflow (~3.0, sample mm-8); HREE depletion is not typical ($Gd_N/Yn_{Nmedian} = 1.2$); Eu anomaly is negative, but its value is relatively low (minimum 0.7, maximum 1.0). In the area located 2 km below the Pinega River (site 3), La_N/Yb_N in bottom sediments increases to 9.3 (sample mm-1, Fig. 7b), and Eu anomaly becomes positive (Eu/Eu* ~1.1). Therefore, we can suppose that bot-

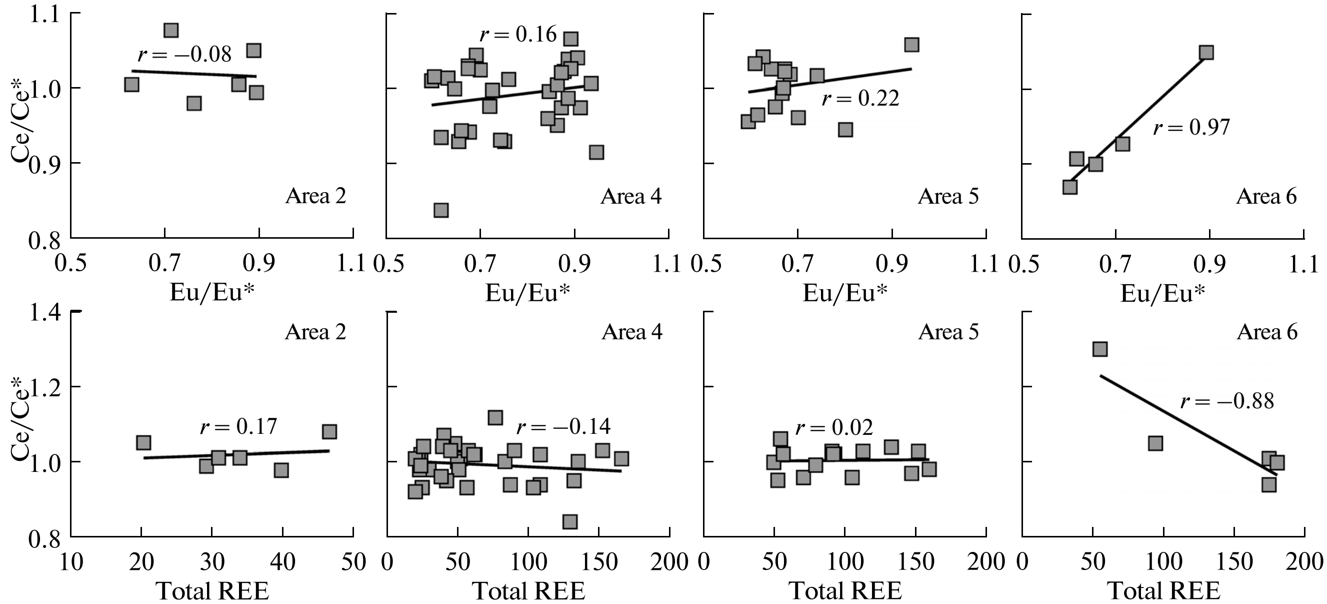

Fig. 8. Eu/Eu*–Ce/Ce* and ΣREE–Ce/Ce* correlation in the most representative (in terms of the number of samples) samplings.

tom sediments of the Pinega River are enriched in the weakly decomposed plagioclase.

In the Severnaya Dvina River delta, $La_N/Yb_{Nmedian} = 7.0$ and sediments are undepleted in HREE ($Gd_N/Yb_{Nmedian} = 1.4$) as in all of the examples discussed above. The Eu anomaly varies from 0.7 to 1.1 (in 21 among 34 analyzed samples, Eu/Eu* is higher than 0.8). In general terms, the above parameters of chondrite-normalized spectra of REE distribution are also retained in recent bottom sediments of the Dvina Bay ($La_n/Yb_{Nmedian} = 7.2$, $Gd_N/Yb_{Nmedian} = 1.4$, Eu/Eu* varies from 0.7 to ~1.1) (Fig. 7d). At the Dvina Bay Basin boundary (site 6), La_N/Yb_N in five analyzed samples varies from 6.0 to 16.2, leading to an appreciable growth of the median value of the given parameter (9.4). Among five samples taken from this area, one sample is distinctly depleted in HREE ($Gd_N/Yb_N = 2.4$).

The chondrite-normalized spectra of REE in samples from the Tersky coast of the Kola Peninsula are also different. This is most prominent with respect to Eu/Eu*: among four samples, the value is lower than 0.8 in two samples and higher than 1.4 in the other two samples (Fig. 7f).

In general, the REE distribution discussed above suggest that the primary fine alumosiliciclastic material was likely predominated by erosion products of basic rocks with a variable (but significant) content of plagioclase serving as Eu concentrator (even with the consideration of the multiple recycling of sedimentary rocks in the cover of the northwestern periphery of the Mezen syncline). At the same time, this conclusion is somewhat inconsistent with La/Sc and Th/Co values suggesting a comparatively acid, granitoid composition of provenance rocks. They could be represented by granodiorites, tonalites, and trondhjemites that are widespread in the basement of the Kola block and the entire northern Russian Platform. It is also evident that the REE spectra of recent bottom sediments in the lower course of the Severnaya Dvina River, Dvina Bay and, apparently, the Basin are comparable within the statistical error limit and, consequently, controlled by the solid discharge of the main water artery in the study region.

Variation of median values of the main parameters of PAAS- and chondrite-normalized REE spectra along the virtual profile extending from site 2 to site 7 (i.e., from the lower course of the Pinega River and the Severnaya Dvina River (sectors above and below the Pinega River mouth) to the Tersky coast of the Kola Peninsula) is shown in Fig. 9. These data indicate that maximal median values of parameters, such as $(La/Yb)_{PAAS}$, $(Gd/Yb)_{PAAS}$, La_N/Yb_N, and Gd_N/Yb_N, are characteristic of samples taken from the Dvina Bay Basin boundary (site 6). In contrast, median Eu/Eu* value here is minimal as at site 5. Median Cr/Th value in bottom sediments is maximal at site 2 and minimal at site 6 (27.1 and 11.2, respectively). Near the Tersky coast of the Kola Peninsula, this parameter is slightly higher than in the central White Sea (Fig. 9c). It should, however, be mentioned that the studied samplings are characterized by significant dispersion probably caused by specific features of the study region: lack of efficient mixing of sediments, considerable influence of the glacial drift on recent bottom sediments of the White Sea, and appreciable contribution

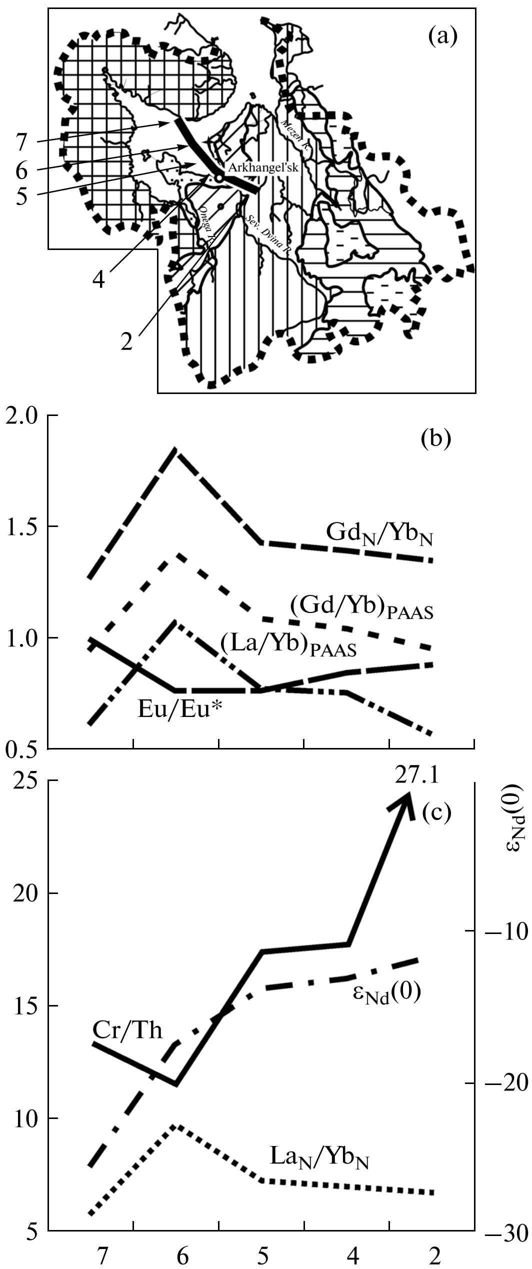

Fig. 9. Schematic positions of the profile and peculiarities of the profilewise variation in the main parameters of REE spectra, Cr/Th (median values), and $\varepsilon_{Nd}(0)$. (a) Schematic position of the profile;(b, c) variations in: (b) Gd_N/Yb_N, $(Gd/Yb)_{PAAS}$, $(La/Yb)_{PAAS}$, Eu/Eu*, (c) Cr/Th, $\varepsilon_{Nd}(0)$, La_N/Yb_N. Other symbols as in Figs. 1 and 5.

of the geochemically more heterogeneous material of tributaries of the Severnaya Dvina River, coastal abrasion (local provenances), and several other factors. This is particularly obvious from the Cr/Th ratio: its standard deviation in samplings from sites 2, 4, and 5 are higher than the average deviation for the sites mentioned above. One can also observe a significant decrease of $\varepsilon_{Nd}(0)$ from site 2 to site 7.

LITHOGEOCHEMISTRY OF SEDIMENTS AND GENETIC RECONSTRUCTIONS

The White Sea is a sufficiently typical epicontinental basin formed in more or less stable tectonic and climatic settings (Nevesskii et al., 1977; *Sistema* ..., 2010; and others). Therefore, the study of recent bottom sediments can provide insight into the response of their bulk chemical composition to several factors (proportions of the influx of lithogenic and petrogenic clastic materials into the basin, paleoclimate, rock in the provenance, and paleotectonic settings of sediments) that control general features of the formation of sedimentary infill in such basins.

Recycling. The long-term redeposition (recycling) of terrigenous sediments promotes their enrichment in the chemically and mechanically mature components: sand and aleurite are enriched in quartz, while pelitic sediments are enriched in illite. According to (Cox et al., 1995; Condie et al., 2001), the relatively low influence of recycling on the formation of fine-grained alumosiliciclastic sediments and sandstones is suggested by the following properties: (1) high K_2O/Al_2O_3 values (0.3–0.4), relatively low Zr/Sc and Th/Sc values in clayey rocks; (2) structural immaturity of psammites; (3) presence of unaltered rock fragments in conglomerate layers associated with psammites and clayey rocks; and (4) presence of sufficiently fresh clastic feldspars in sandstones. The fine-grained terrigenous sediments, which are enriched in the "first cycle" material, are usually marked by the diversed mineral and chemical composition. According to (Yudovich and Ketris, 2000), the "first cycle" rocks are characterized by positive correlation between titanium modulus, TM = TiO_2/Al_2O_3 and iron module, IM = $(FeO + Fe_2O_3 + MnO)/(Al_2O_3 + TiO_2)$, while such correlation is lacking between total alkalinity (natrium–potassium) module, NPM = $(Na_2O + K_2O)/Al_2O_3$ and hydrolyzate module, HM = $(Al_2O_3 + TiO_2 + Fe_2O_3 + FeO + MnO)/SiO_2)$.

The general geological setting suggests that a significant portion of recent bottom sediments of the White Sea was formed from a solid discharge of the Severnaya Dvina River and some smaller rivers that drain the southeastern provenance composed of almost completely sedimentary rocks of the Upper Vendian, Upper Paleozoic, and Mesozoic, i.e., rocks subjected to more than one sedimentation cycle. The bottom sediments are characterized by relatively distinct positive correlation between TM and IM (r = 0.69) and weak correlation between NPM and HM (r = 0.31), supporting the concept about the presence of lithogenic and petrogenic components in the sediments. However, data points of the aleuropelitic and pelitic sediments from the Severnaya Dvina River delta, Dvina Bay, and Dvina Bay Basin boundary in the

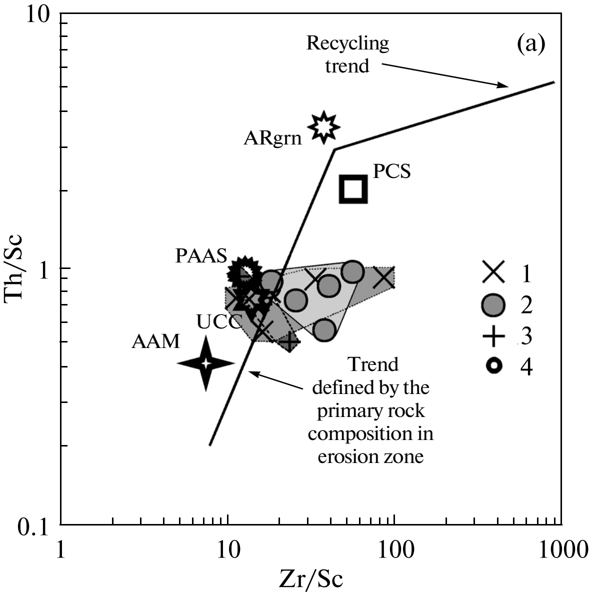

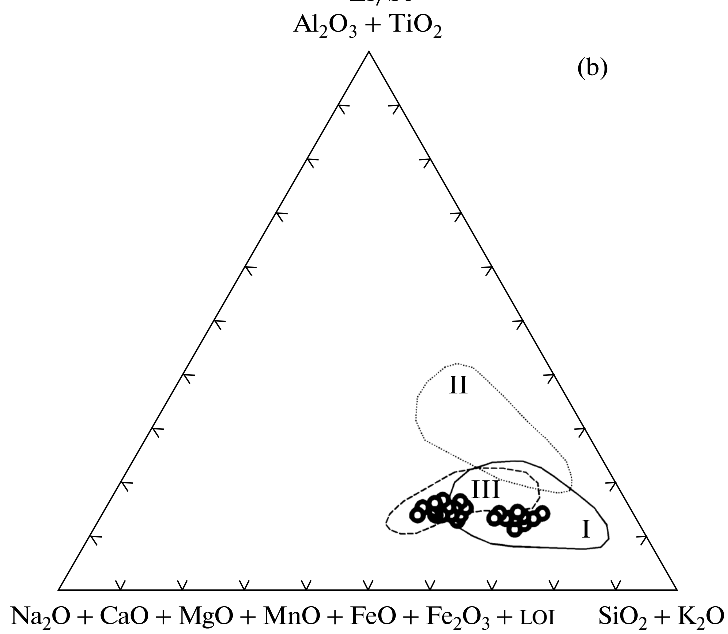

Fig. 10. Distribution of samples of recent bottom sediments of the White Sea in diagrams: (a) Zr/Sc–Th/Sc and (b) Ronov and Khlebnikova. Samples in (a) were taken from: (1) Severnaya Dvina River delta; (2) Dvina Bay; (3) Dvina Bay Basin boundary; (4) recent aleuropelitic and pelitic sediments of the White Sea (Kuz'mina et al., 2009). (PAAS) Average post-Archean Australian shale; (AAM) average Archean mudstone (Taylor and McLennan, 1985); (UCC) upper continental crust (Rudnick and Gao, 2003); (AG) Archean granitoid; (PCS) average Phanerozoic cratonic sandstone (Condie, 1993). Representative fields of: (I) clays in the marine zone, salinated lagoons, and arid zone lakes; (II) continental clays in the tropical zone; (III) continental clays in the cold and moderately cold zones.

Zr/Sc–Th/Sc diagram fall near the trend defined by the primary rock composition in paleocatchment areas (Fig. 10a); i.e., they belong to petrogenic rocks. This is likely caused by more intense (relative to Th) accumulation of Zr in sediments due to a weak preceding recycling and, probably, processes of natural panning.

Paleoclimate. Weathering of rocks in paleocatchment areas, particularly, in humid environment, promotes the removal of dissolved components and the accumulation of the most inert oxides in the weathering crust. The material transformed by weathering is transported to the terminal discharge basins, where its maturity (consequently, intensity of the primary rock transformation in catchment basins) and climate to a certain extent can be assessed based on the bulk chemical composition of sediments. For this purpose, researchers commonly use Al_2O_3/SiO_2 and HM values in kaolinite clays (0.85 and 0.90–0.95, respectively) and hydromicaceous clays (0.33–0.56 and 0.43–0.72, respectively) calculated by the method proposed in (*Metody* ..., 1957), as well as CIA = (100 × $Al_2O_3/(Al_2O_3$ + CaO + Na_2O + K_2O)) (Nesbitt and Young, 1982), CIW = (100 × $Al_2O_3/(Al_2O_3$ + CaO + Na_2O) (Harnois, 1988), and other indexes (Maslov, 2005). Calculation of CIA and CIW values is based on the molecular amounts of oxides. Unweathered and intensely altered rocks are characterized by CIA values of about 50 and as much as 100, respectively. In the weakly altered basalts and granites, CIW varies from 59 to 76; in weathering crust of the above rocks, the value reaches 94–98. It was also shown in (Ronov and Khlebnikova, 1961) that the chemical composition of clays from the continental basins of cold and moderately climate regions bear only insignificant signs of rock weathering. They are characterized by sufficiently high contents of SiO_2, Na_2O, and K_2O, but low contents of Al_2O_3 and TiO_2. In contrast, continental clays of the tropical belt are marked by high contents of Al_2O_3 and TiO_2, but low contents of the majority of other major components. As clays of the first group, clays of salinated lagoons and lakes in the arid zone were formed during insignificant chemical weathering. These authors proposed a triangular (Al_2O_3 + TiO_2)–(Na_2O + CaO + MgO + MnO + FeO + Fe_2O_3 + LOI)–(SiO_2 + K_2O) diagram that shows fields of three clay types indicated above.

The aleuropelitic and pelitic clays of the Severnaya Dvina River delta, Dvina Bay, and Dvina Bay Basin boundary are characterized by medium values of HM = 0.38 ± 0.08 (minimum 0.23, maximum 0.50) and Al_2O_3/SiO_2 = 0.25 ± 0.04 (minimum 0.17, maximum 0.31). Therefore, these sediments can commonly be assigned to hydromicaceous clays, i.e., sediments composed of components relatively weakly altered by weathering in catchment basins. This statement does not contradict their typical moderate CIA values ~3. In the diagram of Ronov and Khlebnikova, data points of recent fine-grained sediments from the White Sea are clustered in domains of marine clays, salinated lagoon clays, and arid lakes, as well as continental clays of cold and moderately cold regions (Fig. 10b). This fact supports our previous conclusion about their relation to rocks formed in a sufficiently cold setting.

Composition of rocks in paleocatchment basins. As emphasized in our previous rocks (Maslov et al., 2009, 2010a, 2011, and others), one of the methods used for its reconstruction is the analysis of several indicator ratios of trace elements (La, Th, Co, Sc, Cr, Ni, V, Zr, and others) typical of the fine-grained terrigenous rocks, because it is believed that their contents and ratios in clayey rocks do not change appreciably during lithogenesis and metamorphism. The elements are relatively low-soluble in water. Therefore, they are transported almost without any loss from provenances to sedimentation basins (Taylor and McLennan, 1985; Wronkiewicz and Condie, 1987; McLennan, 1989; Girty et al., 1994; Cullers, 1995; Jahn and Condie, 1995; Bhat and Ghosh, 2001; *Geochemistry* ..., 2003). This method is based on the following observation: relative to basic rocks, felsic igneous rocks (granites and granodiorites) are characterized by one to two orders of magnitude higher Th/Sc, La/Sc, La/Co, Th/Co, Th/Cr, and V/Ni ratios (*Interpretatsiya* ..., 2001). At the same time, relative to felsic rocks, basic igneous rocks are marked by one to two orders of magnitude higher Cr/Zr, Cr/V, and other indicator ratios. Based on the study of Precambrian pelites of the Kaapvaal craton, it was shown in (Condie and Wronkiewicz, 1990) that relative to Eu/Eu*, La_N/Yb_N or Th/U, the Cr/Th ratio is a significantly more sensitive indicator of rock composition in the provenance. Compositions of rocks in the provenance and type of the eroded upper continental crust also govern to some extent the diversity of REE distribution spectra in post-Archean sedimentary rocks (McLennan et al., 1990). For example, basic igneous rocks are characterized by low LREE/HREE values (<4 or 5) and lack of distinct negative Eu anomaly (Eu/Eu* > 0.85–0.90), while felsic rocks are marked by high LREE/HREE values (>8.0) and distinct negative (<0.85) Eu anomaly (Taylor and McLennan, 1985; McLennan and Taylor, 1991).

In the Gd_N/Yb_N–Eu/Eu* diagram (Taylor and McLennan, 1985), data points of the majority of studied samples cluster in the domain of post-Archean cratonic rocks (Fig. 11a). At the same time, some data points characterized by very low negative Eu/Eu* values or absence of Eu anomaly are confined to the average Archean mudstone (Taylor and McLennan, 1985), for example, samples taken from the lower course of the Pinega River, Severnaya Dvina River area 2 km below the Pinega River mouth, and Severnaya Dvina River delta. Two out of four samples taken from the littoral zone of the Tersky coast (samples m-24 and m-25) are characterized by considerably higher (relative to the average Archean mudstone) positive Eu anomaly. As compared to the average Phanerozoic cratonic sandstone, PCS (Condie, 1993), the overwhelming majority of studied samples have lower Gd_N/Yb_N values and less distinct negative Eu anomaly.

In the Co/Hf–Ce/Cr diagram (Dobson et al., 2001), virtually none of the studied samples fall into the field of erosion products of primitive Archean substrates (Maslov, 2007) (Fig. 11b), although some of them have comparable Ce/Cr values. In most samples of recent bottom sediments from the lower Severnaya Dvina River basin and White Sea, the Ce/Cr value is lower than the PAAS and PCS values, while Co/Hf values are intermediate.

In the Eu/Eu*–Cr/Th diagram (Fig. 11c), virtually all data points of samplings available at our disposal are characterized by Cr/Th values intermediate between those typical of the average Archean mudstone and PAAS. Analysis of samples taken in the lower course of the Pinega River, Severnaya Dvina River delta, Dvina Bay, and Dvina Bay Basin transition zone (Fig. 11d) shows their considerable similar-

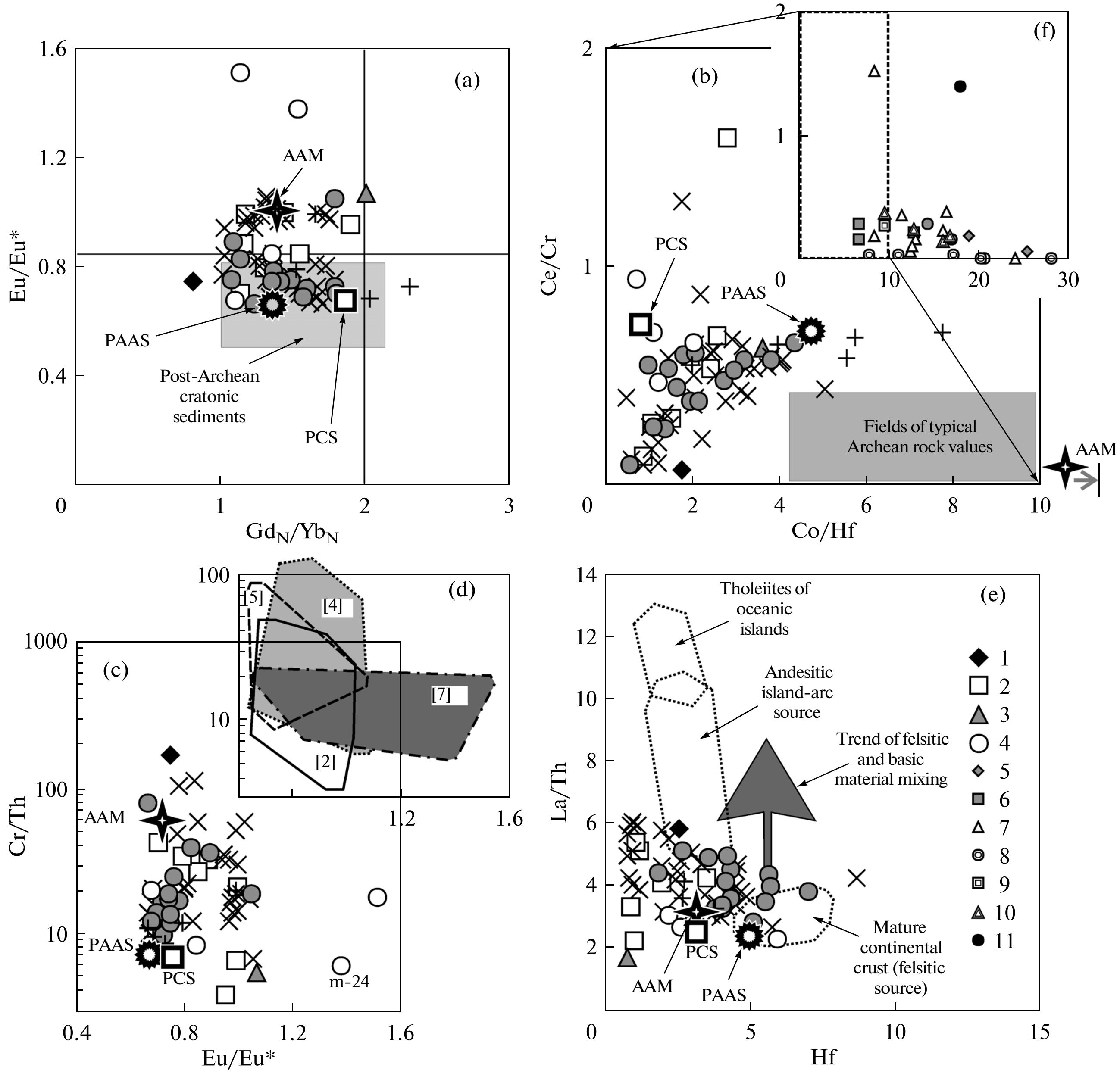

Fig. 11. Distribution of data points of recent bottom sediments in the White Sea and lower course of the Severnaya Dvina River in diagrams: (a) Gd$_N$/Yb$_N$–Eu/Eu*, (b, f) Co/Hf–Ce/Cr, (c, d) Eu/Eu*–Cr/Th, and (e) Hf–La/Th. Sampling sites: (1) Severnaya Dvina River area 20 km away in the Pinega River inflow zone; (2) Pinega River area from the Pinega Settlement to the inflow into the Severnaya Dvina River; (3) Severnaya Dvina River area 2 km below the Pinega River inflow; (4) Tersky coast of the Kola Peninsula at the Varzuga River mouth; (5–11) formations in the Imandra–Varzuga structure (Mints et al., 2010): (5) Kuksha, (6) Purnach, (7) Seidorechensk, (8) Polisarsk, (9) Umba, (10) Il'mozersk, (11) Panarechinsk. Other symbols as in Fig. 10. Fields of typical Archean rock values in Fig. 11a are adopted from (Maslov, 2007); compositional fields in Fig. 11e are adopted from (Gu, 1994; Nath et al., 2000); field numbers in Fig. 11d correspond to areas of profiles: (2) Pinega River area extending from the Pinega Settlement to the river mouth; (4) Severnaya Dvina River delta; (5) Dvina Bay; (7) Tersky coast at the Varzuga River mouth.

ity due to the role of the Severnaya Dvina River as the main supplier of terrigenous material for the White Sea. Owing to high Eu/Eu* in two samples, the composition field of recent littoral sediments from the Tersky coast has a basically different orientation than the fields of other sediments. However, we can assume in the given case that both Archean and post-Archean components are present in sediments of the area under consideration. This fact does not contradict the general geological situation.

Positions of data points of sediments in the Hf–La/Th diagram (Fig. 11e) testify to a leading role of

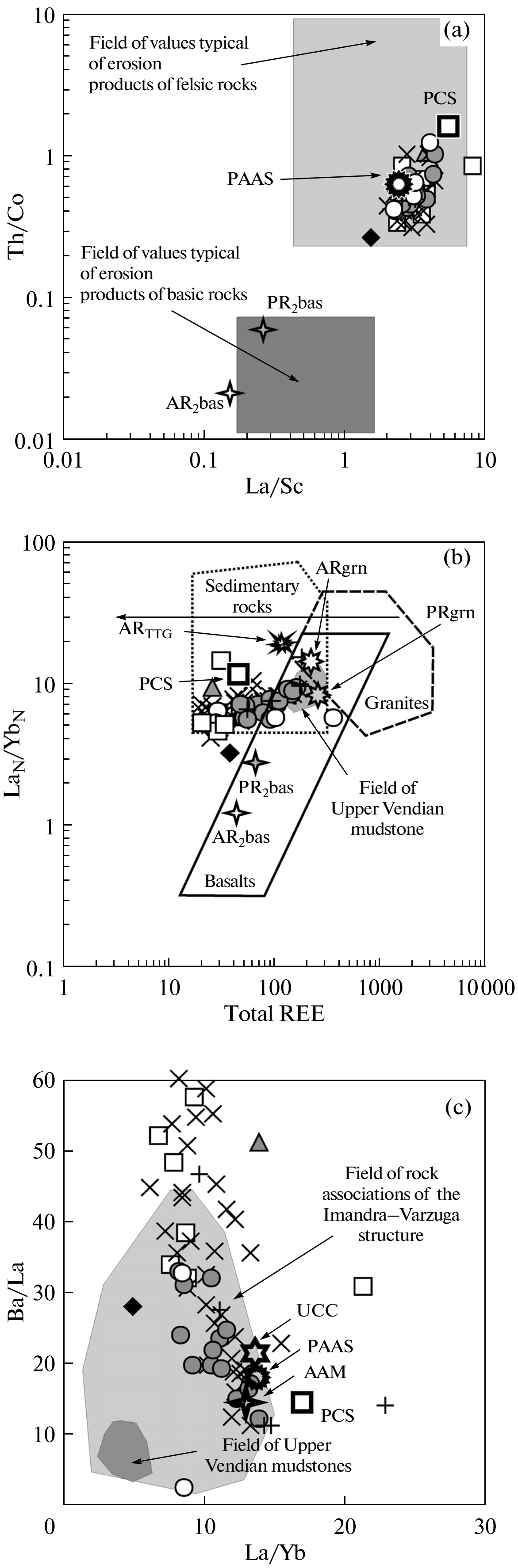

Fig. 12. Distribution of data points of recent bottom sediments of the White Sea and lower course of the Severnaya Dvina River in diagrams: (a) La/Sc–Th/Co, (b) ΣREE–La_N/Yb_N, and (c) La/Yb–Ba/La. Average compositions: (PRgrn) Proterozoic granitoid; (AR_{TTG}) Archean rock of the TTG association; (AR_2bas) Late Archean basalt; (PR_2bas) Late Proterozoic basalt (Condie, 1993). Other symbols as in Figs. 9, 10.

the mature continental crust in the formation of their geochemical signature.

Based on the La/Sc and Th/Co ratios, all of the studied samples can be considered erosion products of felsic igneous rocks (Cullers, 2002) of the PAAS type (Fig. 12a). In the ΣREE–La_N/Yb_N diagram (Allegre and Minster, 1978; Yan et al., 2012), one part of data points of the aleuropelites occurs in the overlap field of basalts and granites in accordance with conclusions based on the REE distribution. Another part is located in the sedimentary rock field similarly as the PCS composition point (Fig. 12b). On the whole, this fact does not contradict the general geological situation. A slightly different pattern is demonstrated by aleuropelite samples in the La/Yb–Ba/La diagram (Kilian and Behrmann, 2003): mainly samples taken from the Dvina Bay and some part of aleuropelites from the Severnaya Dvina River delta are concentrated near data points of PAAS and UCC (Rudnick and Gao, 2003). The remaining samples show a considerably higher Ba/La values (up to 60 or more). In this respect, they are formally similar to pelagic sediments in the Antarctic Plate (Kilian and Behrmann, 2003), although it is yet premature to make genetic conclusions. In terms of La/Yb and Ba/La values, the studied samples of recent bottom sediments in the White Sea and lower course of the Severnaya Dvina River also differ from Vendian fine-grained clastic rocks of the White Sea–Kuloi plateau. At the same time, their significant portion is comparable with rock associations in the Imandra–Varzuga structure of the Kola Peninsula (Fig. 12c).

In Sc/Th–Cr/Th, La_N/Yb_N–Cr/Th, and La_N/Yb_N–Ti/Nb diagrams, data points of aleuropelitic and pelitic sediments of the White Sea and Severnaya Dvina River delta occupy mainly intermediate position between data points of average acid and basic rocks of the Upper Archean and Lower Proterozoic. With respect to several ratios of trace elements, they differ significantly from PAAS, PCS, and AAM, i.e., average Archean mudstone (Taylor and McLennan, 1985) (Figs. 13a, 13b), but they are similar in terms of some other parameters (Fig. 13c).

Values of $\varepsilon_{Nd}(0)$ in samples taken above the Pinega Settlement and in the vicinity of the Orletsy Settlement are –11.7 and –8.5, respectively (Table 3), which are lower than in the fine-grained terrigenous rocks of the Valdai Group (Grazhdankin et al., 2010). This fact likely suggests the erosion of Riphean (?) "juvenile" igneous complexes in the southeastern

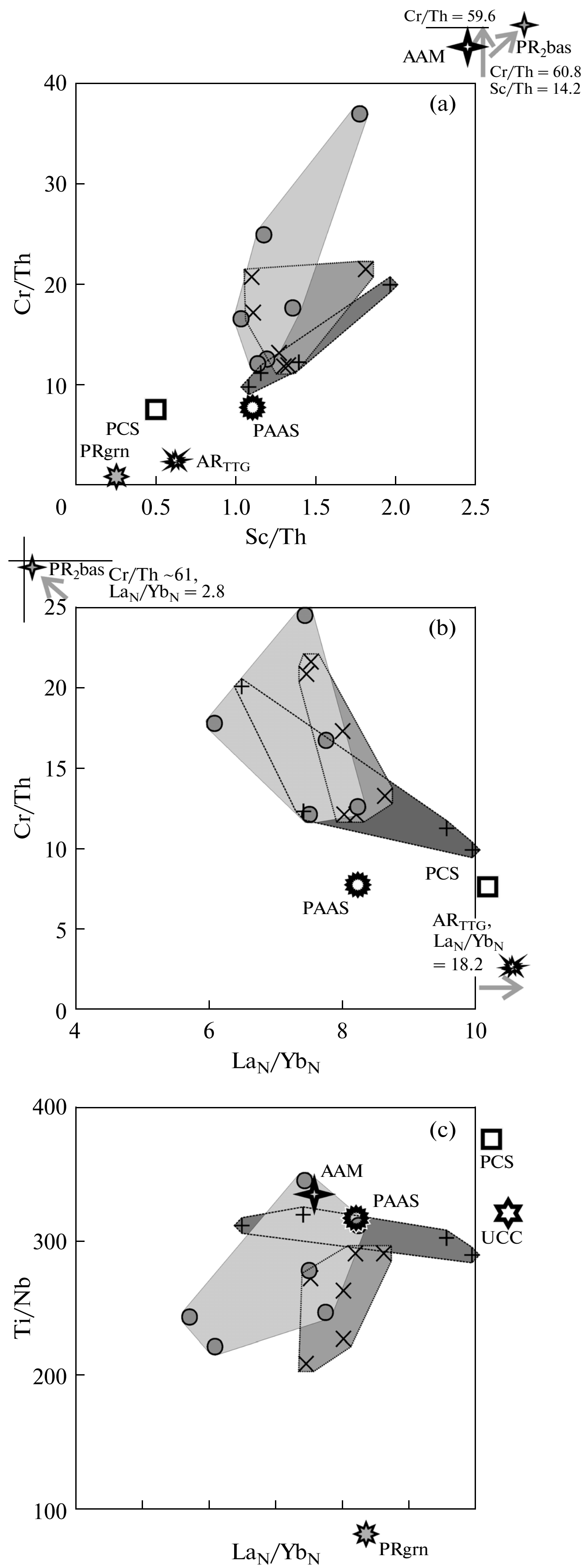

Fig. 13. Distribution of data points of recent aleuropelitic and pelitic sediments of the White Sea and Severnaya Dvina River deltas in diagrams: (a) Sc/Th–Cr/Th, (b) La_N/Yb_N–Cr/Th, and (c) La_N/Yb_N–Ti/Nb. Other symbols as in Figs. 10–12.

provenance in the post-Vendian time. In sediments of the marginal filter of the Severnaya Dvina River, $\varepsilon_{Nd}(0)$ is –13. Bottom sediments taken at the Dvina Bay Basin boundary are characterized by slightly higher $\varepsilon_{Nd}(0)$ (–16.9 and –18.0). Finally, some of the studied littoral sediment samples from the Tersky coast of the Kola Peninsula are marked by two properties that are sharply different from those of both sediments at the marginal filter of the Severnaya Dvina River and sediments of the White Sea Basin. First, they show a prominent (relative to PAAS) positive Eu anomaly. Second, they are marked by the highest $-\varepsilon_{Nd}(0)$ value (–25.6) among the analyzed samples. Our calculated Nd model age (~2.8 Ga) of the lithogenic composition of these sediments is comparable with the median t_{Nd}(DM) value for igneous and supracrustal rocks in the main structural elements of the Baltic Shield (~2.9 Ga) (Grazhdankin et al., 2010) and Nd model age of granite gneisses of the Strel'na block (~2.83 Ga). Value of $\varepsilon_{Nd}(0)$ in bottom sediments of the Severnaya Dvina River above the Pinega River mouth is –8.5. In sediments of the lower course of the Pinega River, Severnaya Dvina River delta, and Dvina Bay, the value varies from –11.7 to –14.6, which do not differ basically from the values reported in (Ronov and Migdisov, 1996) for clayey rocks of the Russian Plate ($\varepsilon_{Nd\ aver}$ – 13.4). All these facts can be attributed to the formation of recent bottom sediments in the White Sea due to the mixing of fine alumosiliciclastic material delivered from the Kola Peninsula and transported by the Severnaya Dvina River.

Redox setting in the near-bottom water layer. Based on Mn and Mo contents in sediments of the Kandalaksha Bay (Strekopytov et al., 2005), we calculated the "stagnation coefficient" (Mo/Mn) that varies from 0.0017 to 0.0034. Criteria suggested in (Kholodov and Nedumov, 1991) indicate that these values testify to the deposition of sediments in a weakly expressed redox setting, but this conclusion does not agree with the concept about a complete oxidation of the upper sediment layer in deep-water zones of the White Sea (Kalinenko, 1975). For more than 75% of the studied samples, Mo/Mn is lower than 0.002 (Fig. 14), suggesting the accumulation of sediments in a sufficiently well-aerated bottom water layer. The stagnation coefficient varies from 0.002 to 0.005 for approximately 21% samples and exceeds 0.01 for less than 2% samples.

Paleotectonic settings. Sandstones formed in different tectonic settings are known to be characterized by appreciable differences in the contents of major petrogenic oxides (Rollinson, 1994; *Interpretatsiya* ...,

Table 3. $\varepsilon_{Nd}(0)$ values in recent bottom sediments of the White Sea and the Severnaya and Pinega rivers

Sample	Sampling location	Sm, ppm	Nd, ppm	$^{147}Sm/^{144}Nd$	±2σ	$^{143}Nd/^{144}Nd$	±2σ	$\varepsilon_{Nd}(0)$
mm-8	1, site 28 (SD-2004)	1.07	5.46	0.1180	0.0006	0.512198	0.000004	–8.5
mm-4	2, site P-1 (SD-2006)	3.77	19.3	0.1185	0.0006	0.512038	0.000003	–11.7
m-36	4, site 64 (SD-2005, may)	5.02	25.5	0.1191	0.0006	0.511959	0.000004	–13.2
m-14	4, site 41 (SD-2006, may)	0.86	4.19	0.1238	0.0006	0.511976	0.000004	–12.9
m-53	5, 0-2 PSh-4925	4.03	20.7	0.1177	0.0006	0.511974	0.000006	–12.9
m-20	5, 0-2 PSh-4684	3.22	16.2	0.1199	0.0006	0.511890	0.000003	–14.6
m-6	6, 0-5 PSh-4698	6.53	33.9	0.1165	0.0006	0.511770	0.000004	–16.9
m-5	6, 0-3 PSh-4697	7.01	37.1	0.1143	0.0006	0.511714	0.000004	–18.0
m-24	7, t. 22 (2008, july)	1.16	5.82	0.1208	0.0006	0.511325	0.000015	–25.6

Sampling location designates areas and sites. Expedition to the estuary of the Severnaya River zone, year, and season are shown in parentheses.

2001; *Geochemistry ...,* 2003; and others). Discrimination of sands and sandstones based on their tectonic settings is accomplished by several binary and ternary diagrams: K_2O/Na_2O–SiO_2/Al_2O_3 (Maynard et al., 1982), ($Fe_2O_3^*$ + MgO)–TiO_2, ($Fe_2O_3^*$ + MgO)–Al_2O_3/SiO_2, ($Fe_2O_3^*$ + MgO)–K_2O/Na_2O, ($Fe_2O_3^*$ + MgO)–Al_2O_3/(CaO + Na_2O), and F1–F2[9] (Bhatia, 1983), and SiO_2–K_2O/Na_2O (Roser and Korsch, 1986). In (Bhatia and Crook, 1986) based on analysis of the distribution of REE and some other trace elements in Paleozoic graywacke sandstones in Australia, several diagrams were proposed for reconstructing the tectonic setting of their accumulation: Ti/Zr–La/Sc, La/Y–Sc/Cr, La–Th–Sc, Th–Sc–Zr/10, and Th–Co–Zr/10. As the charts mentioned above, these diagrams are widely used at present for defining the tectonic setting of terrigenous associations (Das et al., 2006; Deru et al., 2007; Paikaray et al., 2008; Hegde and Chavadi, 2009; El-Rahman et al., 2010; Abu El-Enen, 2011; Descourvieres et al., 2011; and others), including recent bottom sediments of different marine basins (Yan et al., 2007; and others), although the diagrams not always yield results fitting the real geological setting (Maslov et al., 2012b, 2012c).

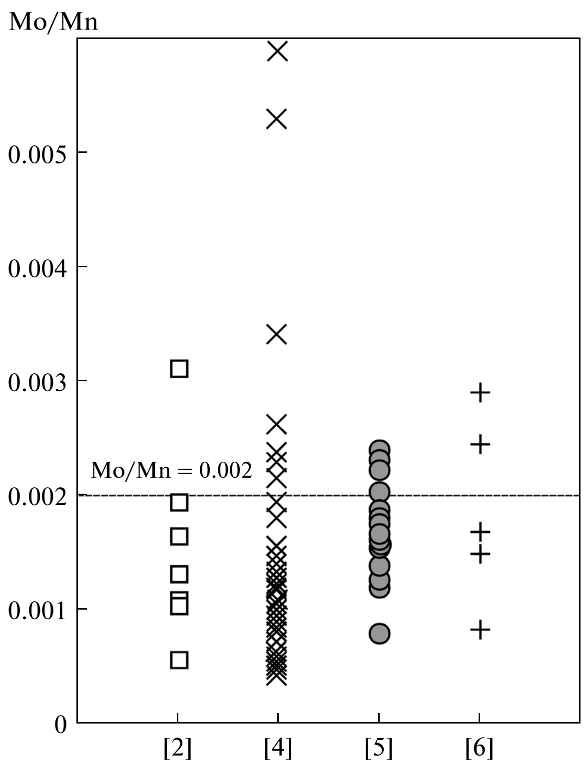

Fig. 14. Distribution of Mo/Mn values in recent bottom sediments of the White Sea and lower courses of the Severnaya Dvina and Pinega rivers. Legend as in Figs. 10 and 11.

We also faced precisely such a situation in our work. In the SiO_2–K_2O/Na_2O diagram, all data points of aleuropelitic and pelitic sediments, which were sampled during cruises 49 and 80 of R/V *Professor Shtokman* in the White Sea (Severnaya Dvina River delta, Dvina Bay, and Dvina Bay Basin boundary) (Kuz'mina et al., 2009), are located in domains typical of sediments associated with oceanic island-arcs (Fig. 15a). Distribution of recent sand, silt, and mud in sediments of the White Sea in the ($Fe_2O_3^*$ + MgO)–Al_2O_3/SiO_2 diagram is also unusual: the overwhelming majority of sand data points cluster in the field of sediments of passive continental margins. On the whole, this observation does not contradict the real

[9] Here, F1 = 0.303 – 0.0447 × SiO_2 – 0.972 × TiO_2 + 0.008 × Al_2O_3 – 0.267 × Fe_2O_3 + 0.208 × FeO – 3.082 × MnO + 0.14 × MgO + 0.195 × CaO + 0.719 × Na_2O – 0.032 × K_2O + 7.51 × P_2O_5; F2 = 43.57 – 0.421 × SiO_2 + 1.988 × TiO_2 – 0.526 × Al_2O_3 – 0.551 × Fe_2O_3 – 1.61 × FeO + 2.72 × MnO + 0.881 × MgO – 0.907 × CaO – 0.177 × Na_2O – 1.84 × K_2O + 7.244 × P_2O_5.

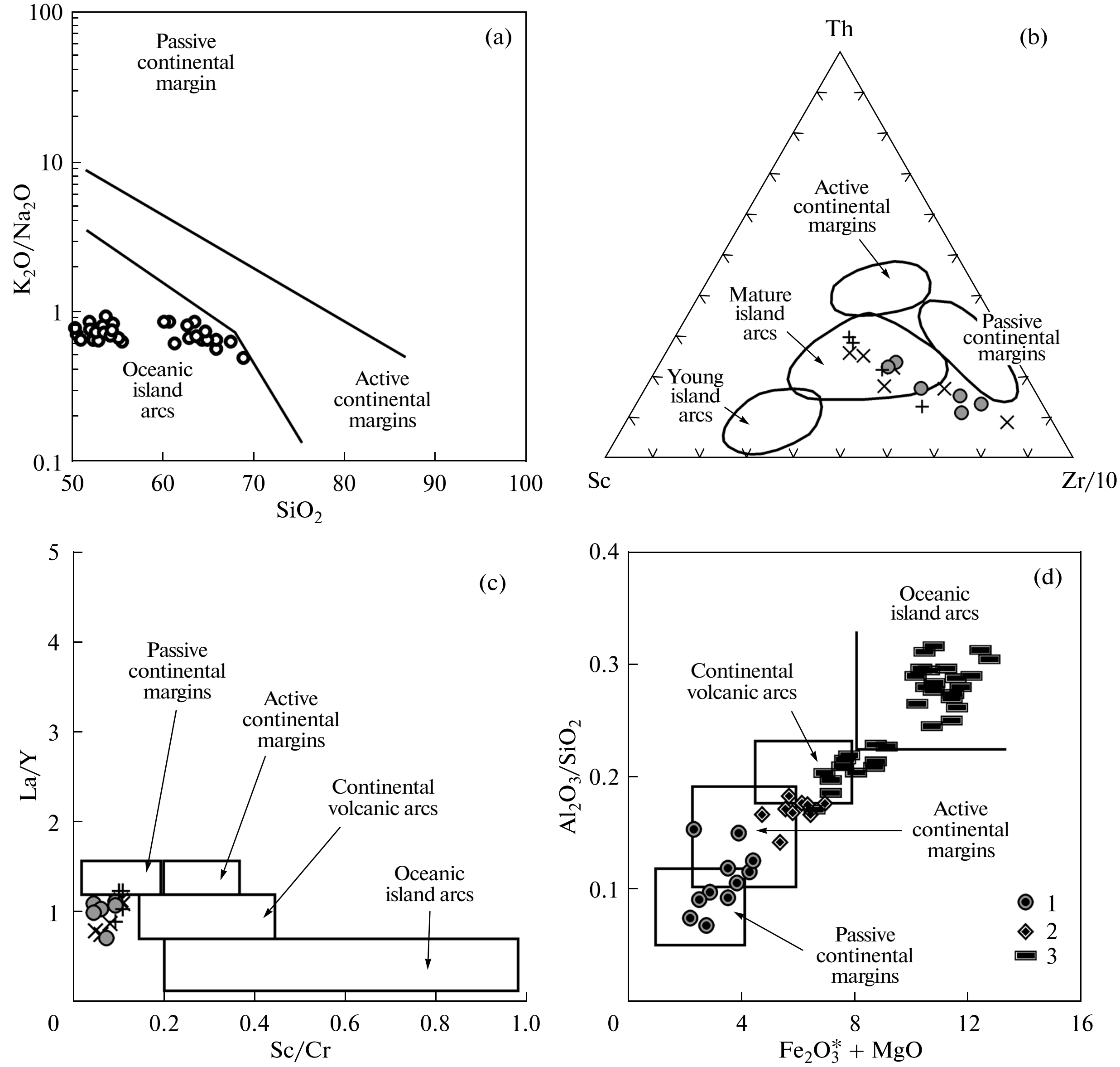

Fig. 15. Positions of data points of aleuropelitic and pelitic sediments of the Severnaya Dvina River delta, Dvina Bay, and Dvina Bay Basin boundary in diagrams: (a) SiO_2–K_2O/Na_2O, (b) Sc–Th–Zr/10, and (c) Sc/Cr–La/Y; (d) distribution of data points of recent sand, silt, and mud of the White Sea in the ($Fe_2O_3^*$ + MgO)–Al_2O_3/SiO_2 diagram (Kuz'mina et al., 2009). (1) Sand; (2) silt; (3) mud. Other symbols as in Fig. 10.

geological situation. In this diagram, silty sediments are located in the field of active continental margins, while data points of mud are located in the fields of continental and oceanic arcs (Fig. 15d) as in the SiO_2–K_2O/Na_2O diagram. In the Sc–Th–Zr/10 diagram, aleuropelitic and pelitic sediments of the Severnaya Dvina River delta, Dvina Bay, and Dvina Bay Basin transition zone cluster both inside and beyond the field of mature island arcs (Fig. 15b). In terms of La/Y values, these samples also match the composition of typical continental volcanic arcs, while Sc/Cr values in them correspond to those of sediments at passive continental margins (Fig. 15c).

We believe that the above situation is related to the following fact: only some of the applied diagrams provide (under certain conditions) reconstruct with a variable degree of probability the formation setting of platformal terrigenous successions. For example, based on the analysis of data on the chemical composition of Upper Proterozoic and Phanerozoic silty–sandy rocks of the Russian Plate reported in (Ronov et al., 1995), we demonstrated that discriminant diagrams proposed by J. Maynard et al. (K_2O/Na_2O–SiO_2/Al_2O_3) and B. Roser and K. Korsch (SiO_2–K_2O/Na_2O) are more reliable for reconstructing the paleotectonic setting of quartz, feldspar–quartz, and arkosic psammites of the platform and subplatform type, whereas diagrams proposed by M. Bhatia—$(Fe_2O_3^* + MgO)–Al_2O_3/SiO_2$, $(Fe_2O_3^* + MgO)–K_2O/Na_2O$, F1–F2, and others—are more suitable for graywackes and compositionally similar sandstones of peri-island arc basins (Maslov et al., 2012b).

CONCLUSIONS

Distribution of average contents of several trace elements (Hf, Sc, Co, Y, Ni, V, Cr, Zr, Ba, and others) in recent bottom sediments from different areas of the White Sea and lower Severnaya Dvina basin shows direct correlation with the amount of the silt-pelite fraction therein. Maximums of the majority of above-listed elements are confined to the silty–pelitic sediments at the Dvina Bay Basin boundary and only some clastophile elements (e.g., Zr and Cr) are located near the White Sea coast. Direct correlation is also observed between the content of silt-pelite fraction in sediments and the total REE content.

Since a significant portion of recent bottom sediments of the White Sea is formed from the solid discharge of the Severnaya Dvina River and its several tributaries that drain the southeastern provenance composed of rocks subjected to more than one sedimentation cycle, one can a priori assume that they should also mainly be composed of lithogenic (several times redeposited) material. This conclusion is in agreement with their bulk chemical composition, but in conflict with geochemical indicators of the recycling of fine alumosiliciclastic material. For example, they belong to petrogenic sediments in terms of Zr/Sc and Th/Sc values typical of the aleuropelitic and pelitic sediments.

Values of HM, Al_2O_3/SiO_2, and CIA typical of aleuropelitic and pelitic muds in the Severnaya Dvina River delta, Dvina Bay, and Dvina Bay Basin transition zone, as well as positions of their data points on the diagram of Ronov and Khlebnikova, suggest that these sediments were formed in sufficiently cold settings.

Lithogeochemical data at our disposal turned out to be insufficient for reconstructing the paleotectonic nature of recent bottom sediments in the White Sea and lower Severnaya Dvina basin. In diagrams of petrogenic oxides, data points of silty–sandy sediments, aleuropelitic, and pelitic sediments are localized in the field typical of sediments associated with oceanic and near-continental island arcs along with passive and active continental margins. Such distribution is likely related, first of all, to the relatively high content of undecomposed or slightly diagenetic transformed petrogenic components, such as plagioclase and ferromanganese minerals (micas, amphiboles, and others), and, secondly, to the influence of hydrogenic factor that promoted the accumulation of Fe and Mn in sediments. In the Sc–Th–Zr/10 diagram, data points of the studied sediments cluster both inside and beyond the field of mature island arcs. In terms of La/Y, these samples correspond to rocks of typical continental volcanic arcs, but Sc/Cr in them corresponds to sediments of passive continental margins.

The PAAS-normalized spectra of REE in bottom sediments of the Pinega and Severnaya Dvina rivers, Severnaya Dvina River delta, Dvina Bay, and Dvina Bay Basin boundary are significantly similar with the REE spectra in clayey rocks of ancient platform cover, but they demonstrate a more distinct positive Eu anomaly. Therefore, we can assume that the REE spectra in recent bottom sediments of the lower Severnaya Dvina basin and White Sea are mainly controlled by the solid discharge of the main water artery in the region (Severnaya Dvina River). This is also indicated by trends of $\varepsilon_{Nd}(0)$ variation in sediments. On the whole, the studied rocks represent sufficiently heterogeneous and not always well-mixed silty–clayey, silty–sandy, and sandy sediments. This is evident from significant variations of $(Eu/Eu^*)_{PAAS}$ and $(La/Yb)_{PAAS}$ even in samples taken from a single area, e.g., Dvina Bay Basin boundary. Samples taken at different sites in cruise 49 of R/V *Professor Shtokman* (Kuz'mina et al., 2009) support this conclusion.

Lack of distinct positive correlation between Eu/Eu* and Ce/Ce*, on the one hand, and Ce/Ce* and total REE, on the other hand, suggests that the postsedimentary transformations of REE spectra are absent in the samples, and they can be used for the reconstruction of rock composition in the catchment basins. Thus, we can assume that erosion products of basic rocks played a certain role in the primary composition of the fine-grained alumosiliciclastic material. At the same time, data on the contents and ratios of some other indicator trace elements suggest alternative conclusions. For example, data on Hf and La/Th in the sediments indicate that erosion products of the mature continental crust played a leading role in the formation of their geochemical signature. This conclusion also follows from their typical La/Sc and Th/Co values. At the same time, data points of recent bottom sediments from the White Sea and Severnaya Dvina River delta occupy an intermediate position between average felsic and mafic rocks of the Archean and Proterozoic in Sc/Th–Cr/Th, La_N/Yb_N–Cr/Th, and La_N/Yb_N–Ti/Nb diagrams.

In general, the distribution of data points of recent bottom sediments in the White Sea and lower course of the Severnaya Dvina River in Gd_N/Yb_N–Eu/Eu* and Eu/Eu*–Cr/Th diagrams and values of several indicator ratios of trace elements suggest the following point: as the distribution of REE, their composition and distribution is governed by the mixing of clastics from two geochemically contrast provenances: the northwestern source zone mainly composed of Archean and Early Proterozoic crystalline complexes and the southeastern source zone almost exclusively composed of Phanerozoic rocks. The role of the southeastern provenance in the formation of sediments was crucial.

The scenario of sedimentation in the peri- or intercontinental setting controlled by a large river system was reconstructed on the basis of lithological data on the Sinemurian–early Pliensbachian and late Pliensbachian–Aalenian stages of the Caucasian basin evolution (Tuchkova, 2007, 2009). With certain reservations, this scenario can likely be extrapolated to the Laptev Sea, eastern Kara Sea, Bay of Bengal, and several other basins. For example, study of specific features of REE distribution in the surficial water of some areas in the Indian Ocean demonstrated that high Nd concentrations coupled with nonradiogenic ε_{Nd} values (from –9.9 to –11.2) in waters of the Bay of Bengal testify with a high degree of probability to the input of Nd mainly from the Asian continent (primarily, due to the erosion of Himalayas) (Amakawa et al., 2000). Influence of the discharge of Ganga–Brahmaputra river system is also felt at the southern continuation of the Bay of Bengal (in the equatorial part of the Indian Ocean), where ε_{Nd} in the surface water layer is –9.7. Data on the Sr–Nd systematics of Holocene and Pleistocene sediments in the Bengal fan also suggest that Pleistocene turbidites are mainly related to the erosion of Himalayas, whereas Holocene sediments are represented by not only the Himalayan material, but also the fine alumosiliciclastic material from Shri Lanka (Kessarkar et al., 2005).

At the same time, model of the sedimentary infill in the Russian intracontinental basin (Caspian Sea) with the consideration of the geological situation is basically different. However, it is rather difficult at present to judge about reasons for this difference without the essential analytical data.

ACKNOWLEDGMENTS

The authors are grateful to academician A.P. Lisitsyn, V.B. Korobov, and A.B. Kotov for valuable suggestions; D.V. Eroshenko, V.A. Zhamoida, S.M. Isachenko, N.K. Fedorova, and crews of R/V *Professor Shtokman*, *Aisberg-2*, and *Akvanaft-2* for assistance in sampling; and V.P. Kazakova and A.N. Rudakova for the grain size analysis.

This work was supported by the Grant for the Support of Leading Scientific Schools (project no. NSh-618.2012.5), the Program of Basic Research of the Presidium of the Russian Academy of Sciences (program no. 23 *Transeuropean Meridional Marine Ecogeochemical Section*), and the Russian Foundation for Basic Research (project no. 12-05-00998).

REFERENCES

Abu El-Enen, M.M., Geochemistry, provenance, and metamorphic evolution of Gabal Samra Neoproterozoic metapelites, Sinai, Egypt, *J. Afr. Earth Sci.*, 2011, vol. 59, pp. 269–282.

Allegre, C.J. and Minster, J.F., Quantitative models of trace element behavior in magmatic processes, *Earth Planet. Sci. Lett.*, 1978, vol. 38, pp. 1–25.

Amakawa, H., Alibo, D.S., and Nozaki, Y., Nd isotopic composition and REE pattern in the surface waters of the eastern Indian Ocean and its adjacent seas, *Geochim. Cosmochim. Acta*, 2000, vol. 64, pp. 1715–1727.

Belyaev, O.A., The oldest basement of the Terskyoi structural zone, in *Geologicheskoe stroenie i razvitie strukturnykh zon Kol'skogo poluostrova* (Geological Structure and Evolution of Structural Zones in the Kola Peninsula), Apatity: GI KolFAN SSSR, 1980, pp. 3–14.

Bhat, M.I. and Ghosh, S.K., Geochemistry of the 2.51 Ga old Rampur pelites, western Himalayas: implications for their provenance and weathering, *Precambrian Res.*, 2001, vol. 108, pp. 1–16.

Bhatia, M.R., Plate tectonics and geochemical composition of sandstones, *J. Geol.*, 1983, vol. 91, pp. 611–627.

Bhatia, M.R. and Crook, K.A.W., Trace element characteristics of graywackes and tectonic setting discrimination of sedimentary basins, *Contrib. Mineral. Petrol.*, 1986, vol. 92, pp. 181–193.

Condie, K.C., Chemical composition and evolution of the upper continental crust: contrasting results from surface samples and shales, *Chem. Geol.*, 1993, vol. 104, pp. 1–37.

Condie, K.C. and Wronkiewicz, D.J., The Cr/Th ratio in Precambrian pelites from the Kaapvaal Craton as an index of craton evolution, *Earth Planet. Sci. Lett.*, 1990, vol. 97, pp. 256–267.

Condie, K.C., Lee, D., and Farmer, G.L., Tectonic setting and provenance of the Neoproterozoic Uinta Mountain and Big Cottonwood Groups, northern Utah: constraints from geochemistry, Nd isotopes, and detrital modes, *Sediment. Geol.*, 2001, vol. 141–142, pp. 443–464.

Cox, R., Lowe, D.R., and Cullers, R.L., The influence of sediment recycling and basement composition on evolution of mudrock chemistry in the southwestern United States, *Geochim. Cosmochim. Acta*, 1995, vol. 59, pp. 2919–2940.

Cullers, R.L., The control on the major- and trace-element evolution of shales, siltstones and sandstones of Ordovician to Tertiary age in the Wet Mountains region, Colorado, U.S.A., *Chem. Geol.*, 1995, vol. 123, pp. 107–131.

Cullers, R.L., Implications of elemental concentrations for provenance, redox conditions, and metamorphic studies of shales and limestones near Pueblo, CO, USA, *Chem. Geol.*, 2002, vol. 191, pp. 305–327.

Daly, J.S., Balagansky, V.V., Timmerman, M.J., et al., Ion microprobe U-Pb zircon geochronology and isotopic evidence supporting a trans-crustal suture in the Lapland Kola orogen, northern Fennoscandian Shield, *Precambrian Res.*, 2001, vol. 105, nos 2/4, pp. 289–314.

Das, B.K., AL-Mikhlaf, A.S., and Kaur, P., Geochemistry of Mansar Lake sediments, Jammu, India: Implication for source-area weathering, provenance, and tectonic setting, *J. Asian Earth Sci.*, 2006, vol. 26, pp. 649–668.

Demina, L.L., Filip'eva, K.V., Shevchenko, V.P., et al., Geochemistry of the bottom sediments in the mixing zone of the Kem' river with the White sea, *Oceanology*, 2005, vol. 45, no. 6, pp. 805–818.

Deru, X., Xuexiang, G., Pengchun, L., et al., Mesoproterozoic-Neoproterozoic transition: geochemistry, provenance and tectonic setting of clastic sedimentary rocks on the SE margin of the Yangtze Block, South China, *J. Asian Earth Sci.*, 2007, vol. 29, pp. 637–650.

Descourvieres, C., Douglas, G., Leyland, L., et al., Geochemical reconstruction of the provenance, weathering and deposition of detrital-dominated sediments in the Perth Basin: the Cretaceous Leederville Formation, south-west Australia, *Sediment. Geol.*, 2011, vol. 236, pp. 62–76.

Dobson, D.M., Dickens, G.R., and Rea, D.K., Terrigenous sediment on Ceara Rise: a Cenozoic record of South American orogeny and erosion, *Palaeogeogr. Palaeoclimat. Palaeoecol.*, 2001, vol. 165, pp. 215–229.

Dokembriiskaya geologiya SSSR (Precambrian Geology of the Soviet Union), Rundkvist, D.V. and Mitrofanov, F.P., Eds., Leningrad: Nauka, 1988.

Dubinin, A.V., *Geokhimiya redkozemel'nykh elementov v okeane* (Geochemistry of Rare Earth Elements in the Ocean), Moscow: Nauka, 2006.

El-Rahman, Y.A., Polat, A., Fryer, B.J., et al., The provenance and tectonic setting of the Neoproterozoic Um Hassa Greywacke Member, Wadi Hammamat area, Egypt: Evidence from petrography and geochemistry, *J. Afr. Earth Sci.*, 2010, vol. 58, pp. 185–196.

Geochemistry of Sediments and Sedimentary Rocks: Evolutionary Considerations to Mineral Deposit-Forming Environments, Lentz, D.R., Ed., *Geol Ass. Canada*, 2003.

Geologicheskaya karta Kol'skogo regiona (severo-vostochnaya chast' Baltiiskogo shchita). M-b 1 : 500000 (Geoloical Map of the Kola Region (Northeastern Baltic Shield). Scale 1 : 500000), Mitrofanov, F.P., Ed., Apatity: GI KNTs RAN, 1996.

Geologicheskaya karta Vostochno-Evropeiskoi platformy i ee skladchatogo obramleniya (v granitsakh byvshego SSSR). Dovendskie obrazovaniya (Geological Map of the East European Platform and Its Folded Framing Within Boundaries of the Former Soviet Union: Pre-Vendian Rocks), Bekker, Yu.R., Ed., St. Petersburg: VSEGEI, 1996.

Girty, G.H., Hanson, A.D., Knaack, C., and Johnson, D., Provenance determined by REE, Th, Sc analyses of metasedimentary rocks, Boyden Cave Roof Pendant, central Sierra Nevada, California, *J. Sediment. Res.*, 1994, pp. 68–73.

Grazhdankin, D.V., Structure and depositional environment of the Vendian complex in the southeastern White sea area, *Stratigr. Geol. Correlation*, 2003, vol. 11, no. 4, pp. 313–331.

Grazhdankin, D.V., Maslov, A.V., Krupenin, M.T., and Ronkin, Yu.L., *Osadochnye sistemy sylvitskoi serii (verkhnii vend Srednego Urala)* (Sedimentary Systems of the Sylvitsa Group: Upper Vendian of the Middle Urals), Yekaterinburg: UrO RAN, 2010.

Gu, X.X., Geochemical characteristics of the Triassic Tethys-turbidites in northwestern Sichuan, China: implications for provenance and interpretation of the tectonic setting, *Geochim. Cosmochim. Acta*, 1994, vol. 58, pp. 4615–4631.

Gubaidullin, M.G., Main information about the geological structure of the eastern catchment area of the White Sea, in *Sistema Belogo morya*. (The White Sea System), Moscow: Nauchnyi Mir, 2010, vol. 1, pp. 40–57.

Harnois, L., The CIW index: a new chemical index of weathering, *Sediment. Geol.*, 1988, vol. 55, nos 3–4, pp. 319–322.

Hegde, V.S. and Chavadi, V.C., Geochemistry of late Archaean metagreywackes from the Western Dharwar Craton, South India: Implications for provenance and nature of the late Archaean crust, *Gondwana Res.*, 2009, vol. 15, pp. 178–187.

Herron, M.M., Geochemical classification of terrigenous sands and shales from core or log data, *J. Sediment. Petrol.*, 1988, vol. 58, pp. 820–829.

Interpretatsiya geokhimicheskikh dannykh (Interpretation of Geochemical Data), Sklyarov, E.V., Ed., Moscow: Intermet Inzhiniring, 2001.

Jahn, B.-M. and Condie, K.C., Evolution of the Kaapvaal Craton as viewed from geochemical and Sm-Nd isotopic analyses of intracratonic pelites, *Geochim. Cosmochim. Acta*, 1995, vol. 59, pp. 2239–2258.

Kalinenko, V.V., Iron in sediments of the White Sea, in *Problemy geologii shel'fa* (Problems of the Geology of Shelf), Moscow: Nauka, 1975, pp. 91–94.

Kessarkar, P.M., Rao, V.P., Ahmad, S.M., Patil, S.K., Kumar, A.A., Babu, G.A., Chakraborty, S., and Rajan, R.S., Changing sedimentary environment during the Late Quaternary: Sedimentological and isotopic evidence from the distal Bengal Fan, *Deep-Sea Res.*, 2005, part 1, vol. 52, pp. 1591–1615.

Kholodov, V.N. and Nedumov, R.I., Geochemical criteria of the appearance of hydrosulfuric contamination in the water of ancient basins, *Izv. Akad. Nauk SSSR, Ser. Geol.,* 1991, no. 12, pp. 74–82.

Kilian, R. and Behrmann, J.H., Geochemical constraints on the sources of Southern Chile Trench sediments and their recycling in arc magmas of the southern Andes, *J. Geol. Soc. (London)*, 2003, vol. 160, pp. 57–70.

Koukina, S., Korneeva, G.A., Ametistova, L., and Bek, T., A comparative biogeochemical study of sediments from Kandalaksha Bay, White Sea, Russian Arctic, *Polar Record*, 2003, vol. 39, no. (211), pp. 357–367.

Kuz'mina, T.G., Lein, A.Yu., Luchsheva, L.N., et al., Chemical composition of surface sediments of the White sea, *Lithol. Miner. Resour.*, 2009, vol. 44, no.2, pp. 103–119.

Lisitsyn, A.P., *Protsessy okeanskoi sedimentatsii* (Processes of Oceanic Sedimentation), Moscow: Nauka, 1978.

Lisitsyn, A.P., Processes in the catchment area of the White Sea: Preparation, transportation, and deposition of material, material flows, and concept of "living catchment area", in *Sistema Belogo morya* (The White Sea System), Moscow: Nauchnyi Mir, 2010, vol. 1, pp. 353–445.

Lisitsyn, A.P., Shevchenko, V.P., Nemirovskaya, I.A., et al., Development of the 4-D oceanography and creation of fundamental principles for the complex monitoring of marine ecosystems (evidence from the White Sea), in *Fizicheskie, geologicheskie i biologicheskie issledovaniya okeanov i morei* (Physical, Geological, and Biological Studies of Oceans and Seas), Moscow: Nauchnyi Mir, 2010, pp. 559–597.

Ludwig, K.R., *A Geochronological Toolkit for Microsoft Excel*, Berkeley Geochronology Center, 2008.

Maslov, A.V., *Osadochnye porody: metody izucheniya i interpretatsii poluchennykh dannykh* (Sedimentary Rocks: Methods of Study and Interpretation of Data), Yekaterinburg: UGGU, 2005.

Maslov, A.V., Archean metaterrigenous rocks: Major geochemical constraints, *Geochem. Int.*, 2007, vol. 45, no. 4, pp. 327–344.

Maslov, A.V., Krupenin, M.T., Ronkin, Yu.L., et al., Fine-grained aluminosiliciclastic rocks in the Middle Riphean stratotype section in the southern Urals: Formation conditions, composition and provenance evolution, *Lithol. Miner. Resour.,* 2004a, vol. 39, no. 4, pp. 357–381.

Maslov, A.V., Ronkin, Yu.L., Krupenin, M.T., et al., The lower Riphean fine-grained aluminosilicate clastic rocks of the Bashkir anticlinorium in the southern Urals: composition and evolution of their provenance, *Geochem. Int.*, 2004b, vol. 42, no. 6, pp. 561–578.

Maslov, A.V., Grazhdankin, D.V., Podkovyrov, V.N., et al., Composition of sediment provenances and patterns in geological history of the Late Vendian Mezen Basin, *Lithol. Miner. Resour.,* 2008a, vol. 43, no. 3, pp. 260–280.

Maslov, A.V., Nozhkin, A.D., Podkovyrov, V.N., et al., *Geokhimiya tonkozernistykh terrigennykh porod verkhnego dokembriya Severnoi Evrazii* (Geochemistry of the Upper Precambrian Fine-Grained Terrigenous Rocks in northern Eurasia), Yekaterinburg: UrO RAN, 2008b.

Maslov, A.V., Grazhdankin, D.V., Podkovyrov, V.N., et al., Provenance composition and features of geological evolution of the Late Vendian foreland basin of the Timan orogen, *Geochem. Int.*, 2009, vol. 47, no. 12, pp. 1212–1233.

Maslov, A.V., Isherskaya, M.V., Krupenin, M.T., et al., Lithogeochemical features of the Riphean fine-grained rocks in the Kama–Bel'sk aulacogen and their Formation conditions, *Lithol. Miner. Resour.*, 2010a, vol. 45, no. 2, pp. 172–200.

Maslov, A.V., Nozhkin, A.D., Podkovyrov, V.N., et al., Clarkes of concentrations of trace elements in the Riphean fine-grained terrigenous rocks of the Uchur-Maya region and the Yenisei Range, *Russian J. of Pacific Geology.*, 2010b, vol. 4, no. 5, pp. 379–397.

Maslov, A.V., Krupenin, M.T., and Kiseleva, D.V., Lithogeochemistry of the fine-grained siliciclastic rocks of the Vendian Serebryanka Group of the Central Urals, *Geochem. Int.*, 2011, vol. 49, no. 10, pp. 974—1001.

Maslov, A.V., Shevchenko, V.P., Ronkin, Yu.L., et al., Systematics of Th, Cr, Hf, Co, and rare-earth elements in modern bottom sediments of the White Sea and lower reaches of the Severnaya Dvina River, *Dokl. Earth Sci.*, 2012a, vol. 443, part 1, pp. 371–376.

Maslov, A.V., Gareev, E.Z., and Isherskaya, M.V., "Standard" discrimination paleogeodynamic diagrams and platformal sandstone associations, *Otechestvennaya Geol.*, 2012b, no. 3, pp. 55–65.

Maslov, A.V., Podkovyrov, V.N., and Gareev, E.Z., Evolution of the paleogeodynamic settings of the formation of the Lower and Middle Riphean sedimentary sequences of the Uchur-Maya region and the Bashkir meganticlinorium, *Russian J. of Pacific Geology*, 2012c, vol. 6, no. 5, pp. 382–394.

Maynard, J.B., Valloni, R., and Ho, ShingJu., Composition of modern deep sea sands from arc related basin, *Geol. Soc. Am. Spec. Publ.*, 1982, no. 10, pp. 551–561.

McLennan, S.M., Rare earth elements in sedimentary rocks: influence of provenance and sedimentary processes. Geochemistry and Mineralogy of Rare Earth Elements, *Reviews in Mineralogy*, Lipin, B.R. and McKay, G.A. Eds., 1989, vol. 21, pp. 169–200.

McLennan, S.M., Taylor, S.R., McCulloch, M.T., and Maynard, J.B., Geochemical and Nd-Sr isotopic composition of deep-sea turbidites: crustal evolution and plate tectonic associations, *Geochim. Cosmochim. Acta*, 1990, vol. 54, pp. 2015–2050.

McLennan, S.M. and Taylor, S.R., Sedimentary rocks and crustal evolution: tectonic setting and secular trends, *J. Geol.*, 1991, vol. 99, pp. 1–21.

Metody izucheniya osadochnykh porod. (Methods for Studying Sedimentary Rocks), Strakhov, N.M., Ed., Moscow: Gosgeoltekhizdat, 1957, vol. 1.

Mints, M.V., Suleimanov, A.K., Babayants, P.S., et al., Deep structure, evolution, and mineral resources in the Early Precambrian basement of East European Platform, in *Interpretatsiya materialov po opornomu profilyu 1-EV, profilyam 4V i TATSEIS* (Interpretation of Materials of the 1-EV Reference, 4V, and TATSEIS Profiles), Moscow: GEOKART, vol. 1.

Nath, B.N., Kunzendorf, H., and Pluger, W.L., Influence of provenance, weathering and sedimentary processes on the elemental ratios of the fine-grained fraction of the bedload sediments from the Vembanad Lake and the adjoining continental shelf, southwest coast of India, *J. Sediment. Res.*, 2000, vol. 70, no. 5, pp. 1081–1094.

Nesbitt, H.W. and Young, G.M., Early Proterozoic climates and plate motions inferred from major element chemistry of lutites, *Nature*, 1982, vol. 299, pp. 715–717.

Nevesskii, E.N., Medvedev, V.S., and Kalinenko, V.V., *Beloe more: sedimentogenez i istoriya razvitiya v golotsene* (The White Sea: Holocene Sedimentogenesis and Evolution History), Moscow: Nauka, 1977.

Paikaray, S., Banerjee, S., and Mukherji, S., Geochemistry of shales from the Paleoproterozoic to Neoproterozoic Vindhyan Supergroup: Implications on provenance, tectonics and paleoweathering, *J. Asian Earth Sci.*, 2008, vol. 32, pp. 34–48.

Perel'man, A.I., *Geokhimiya* (Geochemistry), Moscow: Vysshaya Shkola, 1979.

Peresypkin, V.I., Lukashin, V.N., Isaeva, A.B., and Prego, R., Lignin and chemical elements in the sediments of Kandalaksha Bay (White Sea), *Oceanology*, 2004, vol. 44, no. 5, pp. 698–709.

Petelin, V.P., *Granulometricheskii analiz morskikh donnykh osadkov* (Grain Size Analysis of Marine Bottom Sediments), Moscow: Nauka, 1967.

Pettijohn, F.J., Potter, R., and Siever, R., *Sand and Sandstone,* Heidelberg: Springer, 1972. Translated under the title *Peski i peschaniki,* Moscow: Mir, 1976.

Pokrovsky, O.S., Viers, J., Shirokova, L.S., et al., Dissolved, suspended, and colloidal fluxes of organic carbon, major and trace elements in the Severnaya Dvina River and its tributary, *Chem. Geol.*, 2010, vol. 273, pp. 136–149.

Rannii dokembrii Baltiiskogo shchita (Early Precambrian of the Baltic Shield), Glebovitskii, V.A., Ed., St. Petersburg: Nauka, 2005.

Rock, N.M., Webb, J.A., McNaughton, N.J., et al., Nonparametric estimation of averages and errors for small datasets in isotope geoscience: a proposal, *Chem. Geol.*, 1987, vol. 66, pp. 163–177.

Rollinson, H.R., *Using geochemical data: evaluation, presentation, interpretation*, Essex: London Group UK Ltd, 1994.

Ronov, A.B. and Khlebnikova, Z.V., Chemical composition of the most important clay types, *Geokhimiya*, 1961, no. 6, pp. 449–469.

Ronov, A.B., Migdisov, A.A., and Khane, K., Quantitative regularities in the compositional evolution of silty–sandy rocks of the Russian Plate, *Geochem. Int.*, 1995, no. 3, pp. 312–336.

Ronov, A.B. and Migdisov, A.A., Quantitative regularities in the structure and composition of sedimentary sequences in the East European Platform and Russian Plate and their position among ancient platforms of the world, *Lithol. Miner. Resour.,* 1996, no. 5, pp. 447–469.

Roser, B.P. and Korsch, R.J., Determination of tectonic setting of sandstone–mudstone suites using SiO_2 content and K_2O/Na_2O ratio, *J. Geol.*, 1986, vol. 94, pp. 635–650.

Rozanov, A.G., Volkov, I.I., Kokryatskaya, N.M., and Yudin, M.V., Manganese and iron in the White Sea: Sedimentation and diagenesis, *Lithol. Miner. Resour.*, 2006, vol. 41, no. 5, pp. 483–501.

Rudnick, R.L. and Gao, S., Composition of the continental crust, *Treatise on Geochemistry*, 2003, vol. 3, pp. 1–64.

Shevchenko, V.P., Pokrovsky, O.S., Filippov, A.S., et al., On the elemental composition of suspended matter of the Severnaya Dvina River (White Sea region), *Dokl. Earth Sci.*, 2010, vol. 430, part 2, pp. 228–234.

Sistema Belogo morya (The White Sea System), Lisitsyn, A.P., Nemirovskaya, I.A., and Shevchenko, V.P., Eds., Moscow: Nauchnyi Mir, 2010, vol. 1.

Strekopytov, S.V. and Uspenskaya, T.Yu., Vinogradova E.L., Dubinin A.V. Geochemistry of early diagenesis of sediments of Kandalaksha Bay, of the White Sea, *Geochem. Int.*, 2005, vol. 43, no. 2, pp. 117–130.

Taylor, S.R. and McLennan, S.M., *The Continental Crust: Its Composition and Evolution*, Oxford: Blackwell 1985. Translated under the title *Kontinental'naya kora, ee sostav i evolyutsiya*, Moscow: Mir, 1988.

Timmerman, M.J. and Daly, J.S., Sm-Nd evidence for late Archean crust formation in the Lapland-Kola Mobile Belt, Kola Peninsula, Russia and Norway, *Precambrian Res.*, 1995, vol. 72, pp. 97–107.

Tkachev, Yu.A. and Yudovich, Ya.E., *Statisticheskaya obrabotka geokhimicheskikh dannykh. Metody i problemy* (Statistical Processing of Geochemical Data), Leningrad: Nauka, 1975.

Tuchkova, M.I., Lithology of Lower–Jurassic rocks of the Greater Caucasus (sedimentation, mineral composition, secondary alterations, and paleogeographic and geodynamic consequences), in *Bol'shoi Kavkaz v alpiiskuyu epokhu* (The Greater Caucasus in the Alpian), Leonov, Yu.G., Ed., M.: GEOS, 2007.

Tuchkova, M.I., Lithology of terrigenous rocks in fold zones of the Mesozoic continental margins (Greater Caucasus, Northeast Asia), *Extended Abstract of DSc (Geol.–Miner.) Dissertation*, Moscow: GIN RAN, 2009.

Wronkiewicz, D.J. and Condie, K.C., Geochemistry of Archean shales from the Witwatersrand Supergroup, South Africa: source-area weathering and provenance, *Geochim. Cosmochim. Acta,* 1987, vol. 51, pp. 2401–2416.

Yan, Y., Xia, B., Lin, G., et al., Geochemical and Nd isotope composition of detrital sediments on the north margin of the South China Sea: provenance and tectonic implications, *Sedimentology*, 2007, vol. 54, pp. 1–17.

Yan, B., Yan, W., Miao, L., et al., Geochemical characteristics and provenance implication of rare earth elements in surface sediments from bays along Guangdong Coast, Southeast China, *Environ. Earth. Sci.*, 2012, vol. 65, no. 7, pp. 2195–2205.

Yapaskurt, O.V., *Osnovy kontseptsii razvitiya litologicheskikh issledovanii na sovremennom urovne: Proekt dlya obsuzhdeniya na 6-m Vserossiiskom litologicheskom soveshchanii 2011 goda* (Principles of the Concept of Development of Lithological Studies at the Modern Level: Project for Discussion at the 6th All-Russia Lithological Conference in 2011), Moscow: MAKS Press, 2010.

Yudovich, Ya.E. and Ketris, M.P., *Osnovy litokhimii* (Fundamentals of Lithochemistry), St. Petersburg: Nauka, 2000.

Translated by D. Sakya